

1 Long-term measurements of ice nucleating particles at Atmospheric 2 Radiation Measurement (ARM) sites worldwide

3 Jessie M. Creamean¹, Carson Hume¹, Maria Vazquez¹, Adam Theisen²

4 ¹Department of Atmospheric Science, Colorado State University, Fort Collins, Colorado, 80523, USA

5 ²Argonne National Laboratory, Lemont, Illinois, 60439, USA

6 *Correspondence to:* Jessie M. Creamean (jessie.creamean@colostate.edu)

7 Abstract

8 Ice nucleating particles (INPs) play a critical role in cloud microphysics and precipitation formation, yet long-term, spatially
9 extensive observational datasets remain limited. Here, we present one of the most comprehensive publicly available datasets
10 of immersion-mode INP concentrations using a single analytical method, generated through the U.S. Department of Energy's
11 (DOE) Atmospheric Radiation Measurement (ARM) user facility. INP filter samples have been collected across a broad range
12 of environments—including agricultural plains, Arctic coastlines, high-elevation mountain sites, marine regions, and urban
13 areas—via fixed observatories, mobile facility deployments, and vertically-resolved tethered balloon system operations. We
14 describe the standardized processing and quality assurance pipeline, from filter collection and processing using the Ice
15 Nucleation Spectrometer to final data products archived on the ARM Data Discovery portal. The dataset includes both total
16 INP concentrations and selectively treated samples, allowing for classification of biological, organic, and inorganic INP types.
17 It features a continuous 5-year record of INP measurements from a central U.S. site, with data collection still ongoing. Seasonal
18 and site-specific differences in INP concentrations are illustrated through intercomparisons at -10°C and -20°C , revealing
19 distinct regional sources and atmospheric drivers. We also outline mechanisms for researchers to access existing data, request
20 additional sample analyses, and propose future field campaigns involving ARM INP measurements. This dataset supports a
21 wide range of scientific applications, from observational and mechanistic studies to model development, and provides critical
22 constraints on aerosol-cloud interactions across diverse atmospheric regimes.

23 Short summary

24 This study presents a comprehensive, publicly available ice nucleating particles (INP) dataset from the U.S. Department of
25 Energy Atmospheric Radiation Measurement (ARM) user facility across diverse environments, including Arctic, agricultural,
26 urban, marine, and mountainous sites. Samples are collected via fixed and mobile platforms and processed using a standardized
27 pipeline. The dataset supports observational and modelling analyses of seasonal, spatial, and compositional variability in INPs.

28 **1 Introduction**

29 The formation and microphysical evolution of cloud droplets and ice crystals are strongly influenced by aerosols acting as
30 cloud condensation nuclei (CCN) and ice nucleating particles (INPs). While INP observations remain sparse compared to other
31 aerosol properties, they are essential for understanding aerosol-cloud interactions and their impacts on cloud microphysics and
32 radiative properties. Immersion freezing—where an INP first acts as a CCN before freezing at temperatures above
33 homogeneous freezing (-38°C)—is particularly important for mixed-phase cloud formation (Kanji et al., 2017; Knopf and
34 Alpert, 2023).

35 An aerosol’s ability to serve as an INP depends on temperature, vapor saturation with respect to water and ice, and particle
36 properties such as composition (chemical, mineral, or biological), morphology, and size, all of which are linked to its source
37 (Hoose and Möhler, 2012). Known atmospheric INPs include mineral dust, soil dust, sea spray, volcanic ash, black carbon,
38 and a range of biological particles (e.g., bacteria, fungal spores, pollen, algae, lichens, macromolecules) (e.g., Conen et al.,
39 2011; Creamean et al., 2013, 2019; Cziczko et al., 2017; DeMott, 1990; DeMott et al., 2016, 2018c; Hill et al., 2016; Huang et
40 al., 2021; Kaufmann et al., 2016; Levin et al., 2010; McCluskey et al., 2017; O’Sullivan et al., 2014, 2016). Among natural
41 INPs, mineral dust and biological particles are especially important. Dust is prevalent and typically active below -15°C , while
42 some biological particles, such as specific bacteria, can initiate freezing at temperatures as high as -1.5°C (Després et al.,
43 2012; Huang et al., 2021; Janine Fröhlich-Nowoisky et al., 2016; Schnell and Vali, 1976; Vali et al., 1976). Quantifying total
44 INPs, as well as distinguishing their biological and mineral fractions, provides critical insight into INP sources and atmospheric
45 abundances.

46 Although offline drop freezing assay techniques have been employed for decades, recent intercomparison studies (DeMott et
47 al., 2017, 2018d, 2025a; Lacher et al., 2024; Wex et al., 2015) affirm their effectiveness for ambient INP sampling. These
48 methods are particularly valuable because they often capture INP concentrations across nearly the full heterogeneous freezing
49 temperature range. Their simplicity makes them well-suited for long-term and remote deployments, as filters or other sample
50 types can be easily collected and later analyzed offline. Long-term, multi-year INP records are critical for improving the
51 representation of INP sources and their temporal evolution in earth system models (Burrows et al., 2022). Schrod et al. (2020)
52 presented long-term measurements of deposition and condensation mode INPs from six diverse climatic regions, including the
53 Amazon, Caribbean, central Europe, and the Arctic. Their near-continuous 24-hour samples—analyzed at -20 , -25 , and $-$
54 30°C —spanned over two years in some locations and showed relatively consistent INP concentrations across sites, generally
55 within one order of magnitude. Similarly, Wex et al. (2019) reported comparable INP levels across multiple Arctic coastal
56 sites, though they observed strong seasonal variability spanning several orders of magnitude, largely driven by the presence or
57 absence of snow and sea ice. Freitas et al. (2023) documented a four-year record of Arctic INPs in Svalbard, which peaked
58 during summer in conjunction with increased fluorescent biological particles. Schneider et al. (2021) reported 14 months of
59 INP data from a Finnish boreal forest, showing seasonal alignment with primary biological aerosol particles (PBAPs),

including pollen. Gratzl et al. (2025) further linked seasonal INP fluctuations in the European sub-Arctic to fungal spores, particularly Basidiomycota, over the course of a year.

As recent studies have shown, long-term INP monitoring is especially powerful when integrated with detailed aerosol properties—such as mass concentration, size distribution, chemical composition, and optical characteristics—routinely measured by global in situ monitoring networks. The U.S. Department of Energy’s Atmospheric Radiation Measurement (ARM) user facility is particularly well-suited for this purpose, with fixed sites and extended-duration mobile deployments that span a range of environments from the Arctic to the midlatitudes and the southern hemisphere. While INP measurements have been conducted at various ARM sites in the past, they were primarily user-driven and not part of the baseline measurement suite. These efforts have provided critical insights, including INP closure studies that reveal discrepancies between observed and predicted INPs, highlighting the need for improved parameterizations that may be missing key INP types (Knopf et al., 2021).

Recently, ARM has begun implementing baseline INP measurements at select sites, with coverage growing both spatially and temporally. The most extensive record to date spans nearly five years at ARM’s fixed observatory in Oklahoma, USA. This paper outlines the availability of the valuable datasets at ARM sites, describing the sampling and offline analysis methods, data quality assurance pipelines, and access for the broader scientific community. A key aim is to raise awareness of these resources beyond current ARM users and encourage broader utilization by both experimentalists and modelers.

2 Sample collection and processing

2.1 ARM sites with existing INP measurements

2.1.1 Fixed sites

Locations where INP measurements have been conducted or are currently underway are shown in Figure 1, with corresponding start and end dates, and filter collection frequency, listed in Table 1. For more up-to-date information on ARM observatories, visit <https://www.arm.gov/capabilities/observatories>. Detailed information on INP sampling, including field logs and filter metadata, is available at <https://www.arm.gov/capabilities/instruments/ins>. Filter samples are currently collected on a routine basis approximately every 6 days at two of the three fixed atmospheric observatories: the Southern Great Plains Central Facility in Lamont, Oklahoma (SGP C1; 314 m AMSL, 36.607° N, 97.488° W) and the North Slope of Alaska Central Facility in Utqiagvik, Alaska (NSA C1; 8 m AMSL, 71.323° N, 156.615° W). Routine filter collections began at SGP C1 in October 2020 and are ongoing indefinitely, making it the first site globally with nearly five years of continuous INP measurements. At NSA C1, filter collection commenced in June 2025 and is likewise planned as a long-term effort.

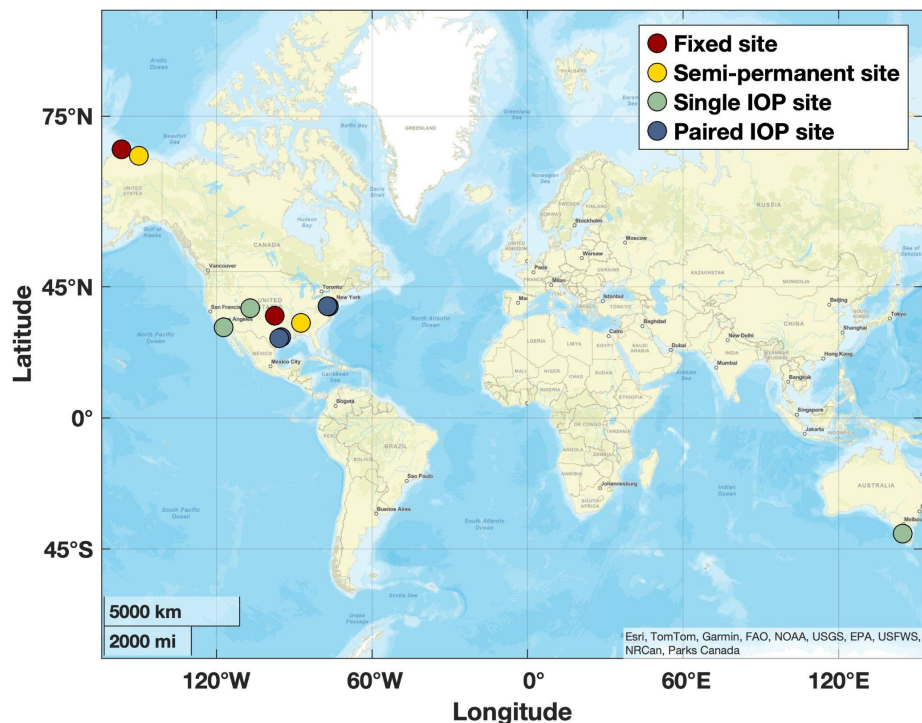


Figure 1. Map of U.S. Department of Energy Atmospheric Radiation Measurement (DOE ARM) user facility sites where routine INP measurements have been established. Red markers show fixed observatories, including Southern Great Plains (SGP C1) and North Slope of Alaska (NSA C1). ARM Mobile Facility (AMF) deployments are shown by yellow markers, while green and blue markers show IOP AMF deployment locations with single and paired sites, respectively. Paired sites indicate IOPs where main and supplemental site locations had simultaneous sample collections. Fixed and semi-permanent sites have single sample collection locations. See Table 1 for site details. Map was generated using Matlab with data from the Environmental Systems Research Institute.

An Intensive Observational Period (IOP) campaign, AGINSGP (Agricultural Ice Nuclei at SGP; Burrows, 2023), was conducted from September 2021 to May 2022. The objective of this deployment was to collect observations to better understand the drivers of variability in INP concentrations at the SGP locale, which are hypothesized to be influenced in part by regional emissions from fertile, organic-rich agricultural soils. Scientific users can submit requests to ARM to implement enhanced sampling strategies—such as increased temporal resolution, additional sampling sites, or entirely new locations—similar to the approach used during AGINSGP. Throughout the campaign, INP filters were collected approximately daily to support case study analyses following the field observations.

Table 1. List of DOE ARM sites with INP measurements. Also included are start and end dates and collection frequency of INP filters. Sites are indicated as either fixed, AMF, or ARM user-requested IOP (Intensive Observing Period). Sites that are continuous are labeled as such in the “INP filter end” column and those with “tbd” indicate an end date has yet to be determined.

Site name	Site type	Site ID	INP filter start	INP filter end	Filter collection frequency
-----------	-----------	---------	------------------	----------------	-----------------------------

Southern Great Plains (SGP) Central Facility	fixed	SGP C1	Oct 2020	continuous	every 6 days
North Slope of Alaska (NSA) Central Facility	fixed	NSA C1	Jun 2025	continuous	every 6 days
Agricultural Ice Nuclei at SGP (AGINSGP)	IOP	SGP C1	Apr 2022	Apr 2022	daily
Oliktok Point (OLI) Main Site	AMF	OLI M1	Aug 2020	Jun 2021	every 6 days
Bankhead National Forest (BNF) Main Site	AMF	BNF M1	Oct 2024	tbd	every 6 days
Surface Atmosphere Integrated Field Laboratory (SAIL) Main Site	AMF	GUC M1	Sep 2021	Oct 2021	every 6 days
Surface Atmosphere Integrated Field Laboratory (SAIL) second Supplemental Facility	AMF	GUC S2	Nov 2021	Jun 2023	every 6 days
TRacking Aerosol Convection interactions ExpeRiment (TRACER) Main Site	AMF	HOU M1	Jun 2022	Sep 2022	daily
TRacking Aerosol Convection interactions ExpeRiment (TRACER) third Supplemental Facility	AMF	HOU S3	Jun 2022	Sep 2022	daily
Eastern Pacific Cloud Aerosol Precipitation Experiment (EPCAPE) Main Site	AMF	EPC M1	Feb 2023	Feb 2024	every 6 days
Cloud And Precipitation Experiment at kennaook (CAPE-k) third Supplemental Facility	AMF	KCG S3	Feb 2023	Oct 2025	every 6 days*
Coast-Urban-Rural Atmospheric Gradient Experiment (CoURAGE) Main Site	AMF	CRG M1	Dec 2024	Nov 2025	every 6 days
Coast-Urban-Rural Atmospheric Gradient Experiment (CoURAGE) second Supplemental Facility	AMF	CRG S2	Dec 2024	Nov 2025	every 6 days
CAPE-K-AEROSOLS	IOP	KCG S3	Feb 2025	Apr 2025	daily

*Filter durations vary due to the INS filter system operating only during clean sector “baseline” sampling periods. As such conditions were not always observed daily, individual 24-hour filter collections typically occur every ~6 days but may be more or less than 6 days depending on site-specific conditions.

2.1.2 Mobile facility sites

Scientific users can propose field campaigns (<https://www.arm.gov/research/campaign-proposal>) to deploy one of ARM’s three Mobile Facilities (AMFs) in undersampled regions around the world. These mobile platforms provide comprehensive atmospheric measurements, including INP filter sampling. Deployments for the first and second mobile facilities (AMF1 and AMF2, respectively) typically span 6–18 months, with the third mobile facility (AMF3) being deployed for up to 5–8 years. Information on ARM INP measurements made at the AMFs is also included in Figure 1 and Table 1.

14 The first INP filters were collected as a part of the AMF3 at the Main Site in Oliktok Point, Alaska (OLI M1; 2 m AMSL,
15 70.495° N, 149.886° W), from August 2020 to June 2021. AMF3 was then relocated to the southeastern United States, where
16 filter collections began in October 2024 at the Main Site in Bankhead National Forest, Alabama (BNF M1; 293 m AMSL,
17 34.342° N, 87.338° W), and are ongoing.

18 INP filters were collected as a part of the AMF2 during the Surface Atmosphere Integrated Field Laboratory (SAIL; Feldman
19 et al., 2023) campaign in Crested Butte, Colorado. Sampling began at the Main Site (GUC M1; 2886 m AMSL, 38.956° N,
20 106.988° W) in September 2021 and continued through October 2021, before transitioning to the second Supplemental Facility
21 on Mt. Crested Butte (GUC S2; 3137 m AMSL, 38.898° N, 106.94° W), where collections continued for the duration of the
22 campaign from November 2021 to June 2023. AMF2 was subsequently deployed to Australia, where INP filters were collected
23 at the third Supplemental Facility during the Cloud And Precipitation Experiment at kennaook (CAPE-k) campaign, located
24 at the kennaook/Cape Grim Baseline Air Pollution Station on the northwestern tip of Tasmania (KCG S3; 67 m AMSL,
25 40.683° S, 144.690° E). This deployment began in February 2023 and concluded in October 2025. These samples were
26 collected during clean sector or “baseline” conditions—when winds originated from the southwest, transporting air masses
27 across the Southern Ocean that were free from local point source contamination. However, select samples were also captured
28 air masses from over Tasmania to help characterize potential local influences. Baseline information indicating when sector-
29 based sampling was active is available through the ARM Data Discovery portal
30 (https://adc.arm.gov/discovery/#/results/instrument_code::baseline).

31 The first INP filters collected using AMF1 were obtained in Texas during the TRacking Aerosol Convection interactions
32 ExpeRiment (TRACER) campaign (Jensen et al., 2023). Filters were collected at both the Main and third Supplemental Facility
33 sites in Houston (HOU M1: 8 m AMSL, 29.670° N, 95.059° W; HOU S3: 20 m AMSL, 29.328° N, 95.741° W) from June to
34 September 2022. The M1 site represented an urban environment, while the S3 site was rural. Due to the short duration of this
35 deployment, filters were collected approximately daily at both locations. Following TRACER, AMF1 was deployed to La
36 Jolla, California, as part of the Eastern Pacific Cloud Aerosol Precipitation Experiment (EPCAPE; Russell et al., 2024), where
37 INP filters were collected at the Main Site (EPC M1; 7 m AMSL, 32.867° N, 117.257° W) from February 2023 to February
38 2024. AMF1 resided in Maryland for the Coast-Urban-Rural Atmospheric Gradient Experiment (CoURAGE), where filter
39 collection occurred at both the Main and second Supplemental Facility sites in the Baltimore region (CRG M1: 45 m AMSL,
40 39.317° N, 76.586° W; CRG S2: 158 m AMSL, 39.422° N, 77.21° W). This deployment began in December 2024 and
41 continued through November 2025. As with TRACER, the M1 and S2 sites represent urban and rural environments,
42 respectively.

43 A very recent IOP campaign, known as CAPE-K-AEROSOLS (CAPE-k Summertime Single-Particle and INP Campaign),
44 was conducted from February to April 2025. This campaign aimed to improve understanding and predictability of Southern

45 Ocean aerosol concentrations, chemical composition, and sources, as well as their relationships to CCN and INPs. During this
 46 period, INP filters were collected approximately daily.

47 **2.1.3 Tethered balloon system (TBS) deployments**

48 ARM operates three TBSs, each capable of carrying payloads up to 50 kg on repeated vertical profiles through the atmospheric
 49 boundary layer, reaching elevations of approximately 1500 m AMSL depending on meteorological conditions and regulatory
 50 constraints. Detailed descriptions of the TBS systems are provided in Dexheimer et al. (2024). Vertically resolved INP filters
 51 have been collected during several ARM TBS deployments through ARM field campaign requests, using a customized
 52 miniaturized sampler. The TBS INP sampler design, filter preparations, deployments, and available data are described in detail
 53 in Creamean et al. (2025) and are only briefly mentioned here.

54 **2.2 Filter preparation and sample collection**

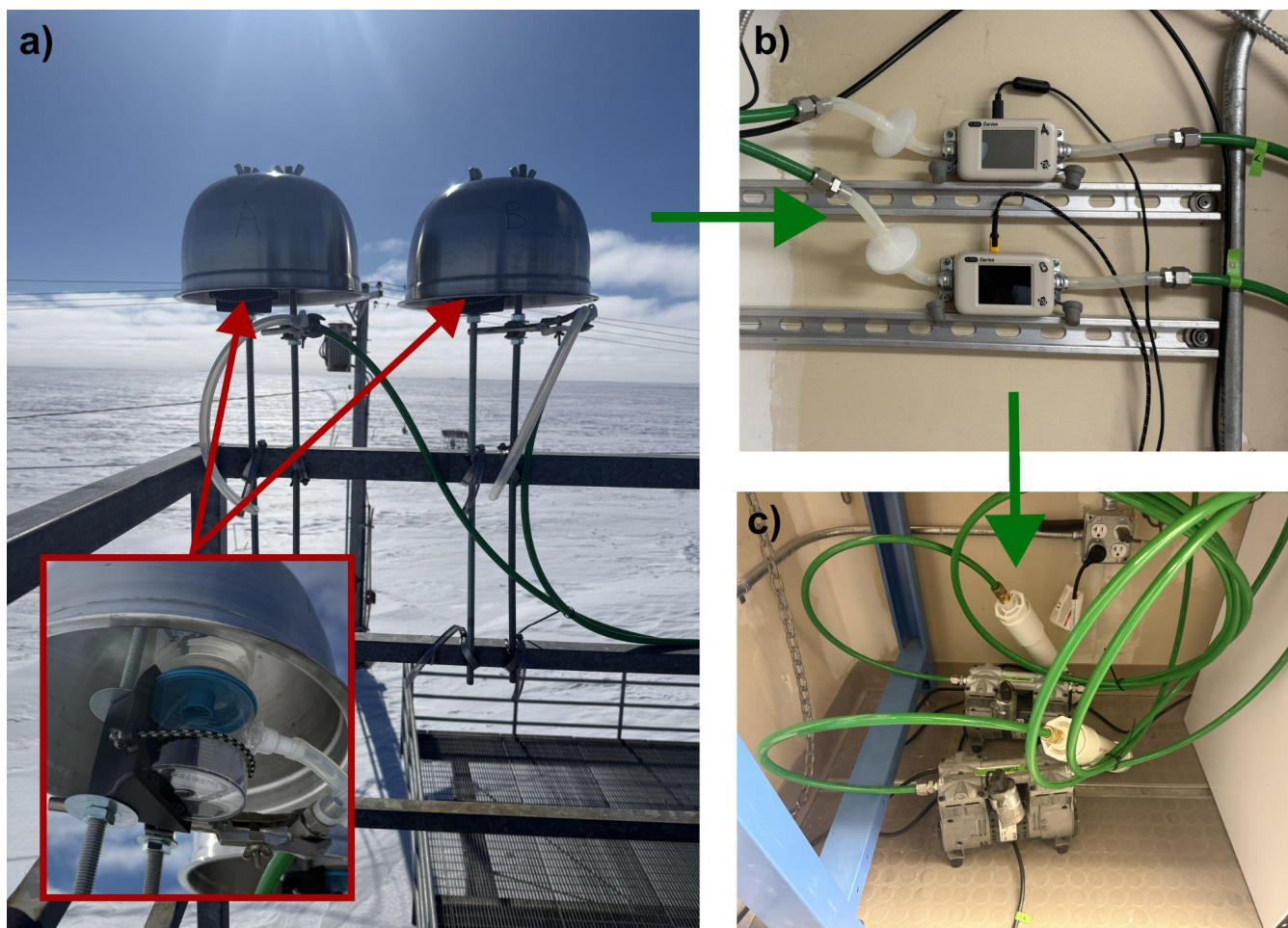
55 **2.2.1 Fixed and AMF locations**

56 Filter units are prepared following the methodology outlined in Creamean et al. (2024), with a brief summary provided here.
 57 Single-use Nalgene™ Sterile Analytical Filter Units are modified by replacing the original cellulose nitrate filters with 0.2-
 58 µm polycarbonate filters, backed by either 10-µm polycarbonate filters (both 47 mm diameter Whatman® Nuclepore™ Track-
 59 Etched Membranes) or 1-µm cellulose nitrate filters (47 mm diameter Whatman® non-sterile cellulose nitrate membranes),
 60 depending on the anticipated aerosol loading at each site. All components are pre-cleaned in-house following the procedure
 61 described in Barry et al. (2021). Filter units are disassembled and reassembled under ultraclean conditions inside a laminar
 62 flow cabinet with near-zero ambient particle concentrations, then sealed and stored individually in clean airtight bags until
 63 deployment.

64 Each sampling setup consists of the sterile, single-use filter units prepared at CSU, a totalizing mass flow meter (TSI Mass
 65 Flow Meter 5200-1 or 5300-1, TSI Inc.), a vacuum pump (Oil-less Piston Compressor/Vacuum Pump, Thomas), connecting
 66 tubing, and precipitation shields (Figure 2). Two identical filter assemblies operate in parallel: one collects primary filters for
 67 INP analysis, while the other collects duplicate filters, which serve either as backups or as archival samples available for user-
 68 requested analysis. The filter units are mounted open-faced and secured to the exterior of the AMF or other fixed-site
 69 infrastructure, protected from precipitation by shield covers. Each unit is connected via vacuum line tubing to the flow meter
 70 and vacuum pump, which are housed either within the main container or in an external pump enclosure, depending on the
 71 available space and site-specific conditions.

72 Upon completion of sampling (typically after 24 hours) the 0.2-µm filters containing the collected aerosol particles are
 73 carefully removed from the single-use filter units and stored frozen at approximately –20 °C in individual sterile Petri dishes
 74 (Pall®). As detailed in Table 1, the 24-hour samples are collected either daily or roughly every 6 days, depending on the goals

75 and duration of the measurement campaign. These samples are preserved on site until they can be transported in frozen batches
76 to CSU, where they remain frozen until they are processed and analysed.



77
78 **Figure 2: Filter unit sampling apparatuses, including a) single-use, open-face filter units under precipitation shields which are**
79 **connected via tubing to b) the mass flow meters and to c) the vacuum pumps.** Flow meters and pumps are always shielded from outside
80 conditions. The inset in a) shows a magnified photo of a filter unit in a custom, 3D-printed filter holder. All photos are from the NSA C1
81 site.

82 2.3 Sample processing with the Ice Nucleation Spectrometer (INS)

83 The INS mimics immersion freezing of cloud ice through ambient aerosols serving as INPs by way of heterogeneous ice
84 nucleation. This technique provides quantitative information on the population of ambient aerosols that can facilitate cloud ice
85 formation at a wide range of subzero temperatures and, hence, INP concentration (e.g., 6 orders of magnitude). The INS (also
86 known as the Colorado State University (CSU) Ice Spectrometer) is supported with well-established experimental protocols
87 and has been applied in many diverse scenarios (e.g., Beall et al., 2017; DeMott et al., 2017; Hill et al., 2016; Hiranuma et al.,
88 2015; McCluskey et al., 2017, 2018; Suski et al., 2018). It is an offline analytical instrument used to quantify freezing

89 temperature spectra of immersion mode INP number concentrations from collected filter samples (Creamean et al., 2024).
90 Each INS unit consists of two 96-well aluminum incubation blocks originally designed for polymerase chain reaction (PCR)
91 plates, positioned end-to-end and thermally regulated by cold plates encasing the sides and base. Two INS instruments are
92 operated side-by-side to increase sample processing throughput. The temperature measurement range of the INS is between 0
93 °C and approximately -27 to -30 °C.

94 For analysis, each filter is placed in a sterile 50 mL polypropylene tube with 7–10 mL of 0.1 µm-filtered deionized water,
95 depending on expected aerosol loading. Lower volumes are used for cleaner environments to improve sensitivity. Samples are
96 re-suspended by rotating the tubes end-over-end for 20 minutes. Dilution series are prepared using the suspensions and 0.1 µm-
97 filtered deionized water, typically including 11-fold dilutions. Each suspension and its dilutions are dispensed into blocks of
98 32 aliquots (50 µL each) in single-use 96-well PCR trays (Optimum Ultra), alongside a 32-well negative control of filtered
99 deionized water. The trays are placed in the aluminum blocks of the INS and cooled at 0.33 °C min⁻¹. Freezing is detected
00 optically using a CCD camera with 1-second data resolution. HEPA-filtered N₂, pre-cooled near block temperature,
01 continuously purges the headspace to prevent condensation build-up and warming of the aliquots.

02 The time between collection and analysis has ranged from one week to over a year. Beall et al. (2020) reported no significant
03 differences in INP concentrations for samples stored between 1 and 166 days. In our internal quality checks, select samples
04 stored for 1–2.5 years at -20 °C showed minimal differences (<1%), while larger differences (20–60%) were observed only in
05 outlier cases associated with problematic original measurements.

06 **2.3.1 Heat and peroxide treatments**

07 Thermal and hydrogen peroxide (H₂O₂) treatments are used to probe INP composition, specifically targeting biologically-
08 derived materials (Maki et al., 1974). Heat treatment involves heating 2.5 mL of sample suspension to 95 °C for 20 minutes to
09 denature heat-labile INPs, such as proteins (Barry et al., 2023b, a; Hill et al., 2016, 2023; McCluskey et al., 2018b, c, a; Moore
10 et al., 2025; Suski et al., 2018; Testa et al., 2021). Peroxide digestion is performed on a separate 2 mL aliquot by adding 1 mL
11 of 30% H₂O₂ (Sigma-Aldrich®) to deionized water to create a 10% solution, followed by heating to 95 °C for 20 minutes
12 under UVB illumination to generate hydroxyl radicals. Residual H₂O₂ is then neutralized using catalase (MP Biomedicals™,
13 bovine liver). This process removes bio-organic INPs, as detailed in McCluskey et al. (2018c), Suski et al. (2018), and Testa
14 et al. (2021). H₂O₂ has long been used as an oxidizing agent for degrading organic matter, originating in soil science nearly a
15 century ago and later adopted across disciplines for removing organic material prior to chemical or physical analyses (McLean,
16 1931; Mikutta et al., 2005; Robinson, 1922; Schultz et al., 1999; Sequi and Aringhieri, 1977). In the presence of UV light,
17 H₂O₂ photolyzes to form highly reactive hydroxyl radicals that can oxidize and structurally modify organic macromolecules,
18 diminishing or eliminating their ice-nucleating activity (DeMott et al., 2023; Gute and Abbatt, 2020). Within the INP
19 community, H₂O₂ treatments typically range from 10 to 35% (Beall et al., 2022; O’Sullivan et al., 2014; Perkins et al., 2020;

Roy et al., 2021; Teska et al., 2024; Tobo et al., 2019). We conducted recent tests showing minimal differences in ice-nucleating activity between 10% and 20% treatments; however, further validation is needed, and future community efforts should aim to establish a standardized protocol and concentration to ensure methodological consistency across studies.

The differences in freezing spectra before and after each treatment provide insights into INP composition—yielding total, heat-labile (biological), bio-organic, and inorganic (often mineral) INP concentrations. However, it is important to note that wet heating may lead to a slight decrease in ice nucleation activity in select mineral types (Daily et al., 2022). Blanks are included during peroxide digestion to monitor potential contamination from reagents. Treatments are typically applied to one-third of samples from each location. Due to the ongoing nature of this program, the numbers of treatments conducted on samples from any given site evolve continuously on a weekly basis. Exact sample sites, dates, identifiers, and other metadata regarding which samples undergo treatments can be accessed in real time via the publicly available field log on the INS website. In the data files available on the ARM Data Discovery portal, treatments are indicated by a flag: 0 for base/untreated data, 1 for heat-treated data, and 2 for peroxide-treated data.

3 From raw data to final product: processing and quality control

3.1 INP concentration and uncertainty calculations

INP concentrations are calculated at each temperature interval using the fraction of frozen droplets and the known total volume of air filtered, following Equation (1) (Vali, 1971):

$$K(\theta) \text{ (L}^{-1}\text{)} = \frac{\ln(1-f)}{V_{drop}} \times \frac{V_{suspension}}{V_{air}} \quad (1)$$

where f is the proportion of frozen droplets, V_{drop} is the volume of each droplet, $V_{suspension}$ is the volume of the suspension, and V_{air} is the volume of air sampled (liters at standard temperature and pressure (STP) of 0 °C and 101.32 kPa). Specifically, the $V_{suspension}$ is the volume of 0.1 µm-filtered deionized water used to resuspend the particles from the filter (7–10 mL). The primary output of the INS is the freezing temperature spectrum of cumulative immersion mode INP number concentration, $K(\theta)$, from aerosols re-suspended from individual filters. INS output includes freezing temperature (°C), INP number concentration (L⁻¹ STP), 95% confidence intervals, and a treatment flag. Binomial confidence intervals are calculated following Agresti and Coull (1998), varying with the proportion of wells frozen. For example, freezing in 1 of 32 wells yields a confidence interval range of ~ approximately 0.2–5.0 times the estimated concentration, while 16 of 32 yields approximately 0.7–1.3 times the estimated concentration. The treatment flag denotes whether the suspension was base/untreated (total INPs; a flag of 0), heat-treated (biological INPs deactivated; a flag of 1), or H₂O₂-treated (organic INPs removed; a flag of 2). These values are derived from preliminary data files that include the processing date and time, freezing temperatures, and number of wells frozen (typically out of 32, each containing a 50 µL aliquot) per 0.5 °C interval.

49 Beyond Agresti and Coull confidence intervals, additional systematic and volumetric uncertainties associated with the INP
50 measurements include instrumental and procedural sources that contribute to the overall error budget. The flow meter accuracy
51 is $\pm 4\%$, based on the TSI 5200 Series Gas Flow Meter Operation and Service Manual. Type T thermocouples have an estimated
52 absolute accuracy of $\pm 0.5\text{ }^{\circ}\text{C}$, though the relative uncertainty between data points is closer to $\pm 0.1\text{ }^{\circ}\text{C}$ (Perkins et al., 2020),
53 and no measurable block temperature gradients have been observed in prior laboratory tests. Uncertainties in droplet and
54 suspension volumes arise from pipetting and dispensing variability: $\pm 1.3\%$ for the larger pipette used in dilutions, $\pm 2.5\%$ for
55 the smaller pipette, $\pm 1.8\%$ for the multipipetter, and $\pm 0.1\text{--}0.8\%$ for syringe-dispensed suspension volumes determined via
56 gravimetric testing at CSU. Additionally, edge cases in freezing data (0/32 and 32/32) are not reported, and limits of detection
57 (LOD) vary by sample based on total air and suspension volumes, with values below detection reported as -9999 .

58 **3.2 Quality control and assessment**

59 To ensure the reliability and robustness of immersion freezing data from the INS, we implement a comprehensive quality
60 control and assessment pipeline (Figure 3). This includes field sampling protocols, lab procedures, data validation, and
61 instrument maintenance.

62 **3.2.1 Field sampling quality control**

63 Filter samples collected for offline INS processing are carefully monitored during field deployment. At both the start and end
64 of each sampling period, the in-line pressure (kPa) and flow rate (standard liters per minute; Slpm) are recorded. These values
65 are evaluated for anomalies such as significant pressure or flow changes, which may indicate issues like leaks in the filter unit,
66 tubing, or system connections. To ensure accurate total air volumes are recorded, a totalizing mass flow meter logs flow every
67 second during sample collection. This meter is annually sent to the manufacturer for recalibration. Units that deviate by more
68 than 5% are returned to the manufacturer for servicing and recalibration. Field blanks are also prepared by briefly exposing
69 unused filters to ambient air at the sampling site. All sites undergo field blank collection approximately once per month, with
70 the exception of OLI M1, which is detailed in a Data Quality Report (DQR) that can be viewed under the “Description” for
71 this site’s INP data on the ARM Data Discovery Portal. Moving forward, all existing and new sites in the program will include
72 routine monthly field blanks.

73 Routine maintenance for the field filter sampling system includes: (1) checking in-line temperature, pressure, and flow rate at
74 the beginning and end of each sampling period, (2) inspecting precipitation shields and cleaning them as necessary, (3) ensuring
75 single-use filter units are leak-free before deployment, (4) examining tubing and connection points for blockages or leaks, (5)
76 verifying the performance of the vacuum pumps, which should sustain a 0.5 kPa vacuum, and (6) annual recalibration of the
77 flow meters.

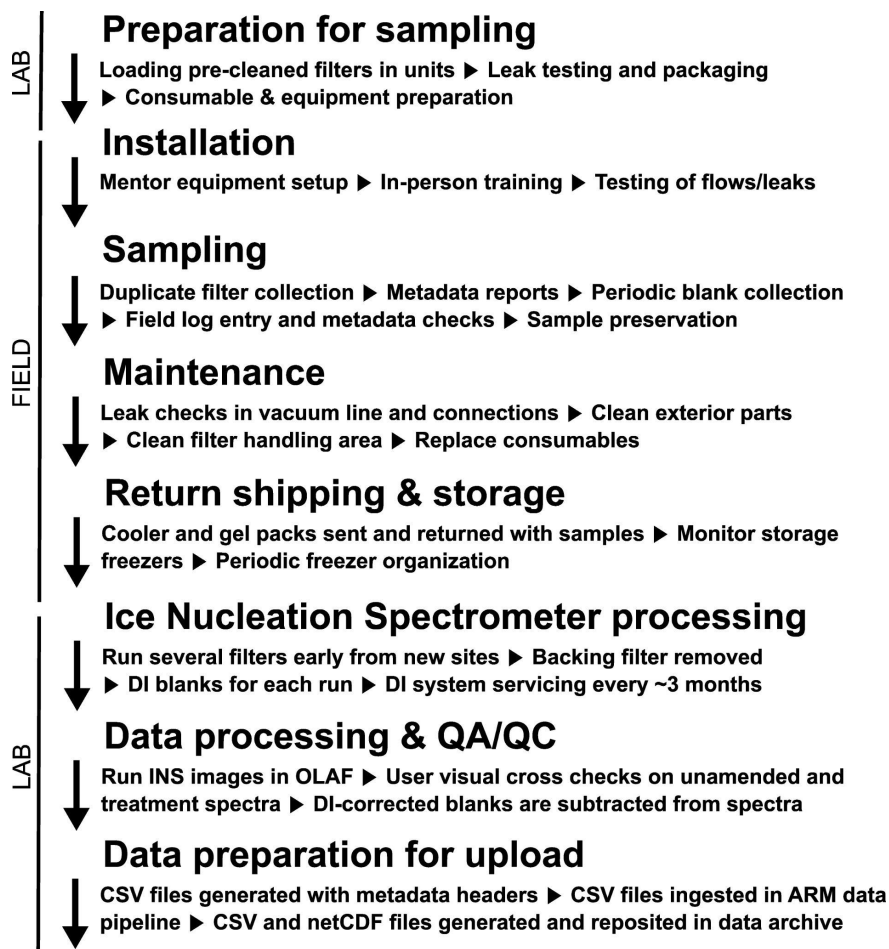


Figure 3: Flow diagram of quality assurance / quality control (QA/QC) protocols designed for DOE ARM INP data. Quality assurance ensures that data meet established standards for both ARM management and scientific end users, while quality control involves systematic inspection and testing to verify that performance characteristics align with predefined specifications. DI = deionized.

3.2.2 Laboratory protocols

To minimize contamination from lab surfaces or consumables (e.g., pipet tips, PCR plates, tubes), we follow a stringent sample preparation protocol (Barry et al., 2021). Pipets are calibrated annually, and a 0.1- μm filtered deionized water blank is included with each INS run to correct for background INPs introduced during re-suspension or by the trays themselves. For peroxide digestion experiments, blanks with deionized water are included to detect potential contamination from H_2O_2 or catalase reagents. These are prepared using the same procedures as the actual samples to assess background INP levels and serve as a quality control check to determine whether reprocessing is necessary.

3.2.3 Instrument quality control and calibration

INS temperature accuracy is critical and maintained within ± 0.2 °C, accounting for thermocouple uncertainty and ensuring no block temperature gradients develop over time. Each PCR block contains one thermocouple inserted just below the wells, and for each pair of blocks, the thermocouple readings are averaged. HEPA-filtered N₂ used to purge the PCR tray headspace is pre-cooled to prevent condensation build-up on plexiglass lids and warming the 50 μ L aliquots during measurement. Camera images are captured every 20 seconds (approximately every 0.1 °C) during analysis to verify automated freezing detection. Each INS run is manually cross-checked against the recorded images to ensure proper identification of frozen wells. The deionized water blanks run with every sample serve a dual purpose: they act as a positive control as well and help monitor instrument drift, potential contamination, and the proper functioning of INS components (e.g., thermocouples, cameras). Routine lab maintenance of the INS includes: (1) cleaning plexiglass lids biweekly with Windex and deionized water, (2) monthly deep cleaning of the lab space, (3) monitoring copper piping for leaks of SYLTHERM™ XLT heat transfer fluid, and (4) watching the nitrogen tank depletion rate to detect leaks. We have confirmed the repeatability and reliability of the INS technique through replicate filter testing and campaign comparisons. Additionally, replicate filters have been analyzed to ensure comparability (Creamean et al., 2024).

3.3 Automated data processing algorithm

Historically, data produced by the INS have been analyzed manually using Microsoft Excel. In 2024, a data scientist was hired to develop the Open-source Library for Automating Freezing Data acQuisition from Ice Nucleation Spectrometer (OLAF DaQ INS), which now has its Version 1 completed. More information and the software itself are available at: <https://github.com/SiGran/OLAF>. Briefly, the OLAF DaQ INS software provides a graphical user interface that allows users to manually cross-check camera images taken during each INS run against the recorded well freezing data. Once image verification is complete, the program generates a CSV file with freezing data at every 0.5 °C interval, including the first instance of observed freezing to the nearest 0.1 °C. PCR wells containing deionized water are automatically subtracted from the sample wells for both the neat and serially diluted suspensions. These deionized water-corrected well freezing data are then converted to INP concentrations (per liter of air at STP) at each temperature bin using Equation (1). Binomial confidence intervals are calculated following Agresti and Coull (1998) and also converted to INP L⁻¹ using the same equation. For each temperature bin, the program selects the INP concentration from the least dilute sample that remains statistically valid. When a dilution reaches its statistically significant limit, the program moves to the next most dilute sample.

In cases where INP concentrations decrease with decreasing temperature (an artifact sometimes introduced by the stochastic nature of serial dilution measurements) the program automatically adjusts the values to enforce monotonicity. We are currently developing an additional QC flag for OLAF-generated data files to indicate which data points were adjusted due to monotonicity-related corrections. This correction was not applied prior to OLAF when files were generated manually. Because blank subtraction can also produce this artifact, the correction is applied after the blank subtraction step. Specifically, if a

21 blank-corrected value falls below the lower 95% confidence bound of the uncorrected value, the program replaces it with the
22 previous bin's value and propagates the upper confidence interval using the root mean square of the current and previous
23 intervals. This correction is applied only when the number of affected bins remains below a user-defined threshold (10% of
24 total temperature bins per sample); if exceeded, those bins are flagged with an error signal (−9999). At ground-based terrestrial
25 sites, corrections are almost entirely due to dilution stochasticity and rarely result from blank subtraction, whereas marine or
26 other low-aerosol loading environments tend to experience a higher frequency of corrections related to blank subtraction.
27 Finally, the software compiles all blank-corrected data across treatments (base/untreated, heat, and peroxide) into a single
28 output file, including treatment flags for each sample.

29 **3.4 Ingesting processed INP data into ARM Data Discovery**

30 The final step in making INS-derived INP data publicly available is ingestion into the ARM Data Discovery portal. This begins
31 with the CSV files generated during INS processing, which are passed through an automated pipeline that standardizes them
32 into a universal format used across all ARM datasets. This format includes all necessary metadata headers and timestamps.
33 During ingestion, the ARM Data Quality Office (DQO) evaluates the data by reviewing plots and statistical metrics of the INP
34 data. If any issues are identified, the DQO works with the mentor team to resolve them. This dual-level review, by both
35 scientific mentors and the DQO, ensures the robustness and reliability of the final data products. Once approved, the data are
36 published at the “a1” level, which denotes that calibration factors have been applied, values have been converted to geophysical
37 units, and the dataset is considered final. These files are available in NetCDF and/or ASCII-CSV formats and can be accessed
38 by placing a data order through the ARM Data Discovery portal. A free ARM account is required to request and download the
39 data.

40 **4 Applications of ARM INP data**

41 **4.1 Temporal trends in INP concentrations from long-term monitoring**

42 As the first established fixed site, SGP C1 hosts nearly five consecutive years of INP concentration data (Figure 4). Untreated
43 (i.e., base, or total INP) measurements, collected approximately every six days, are publicly available. Long-term datasets such
44 as this are invaluable for examining the annual cycle of INPs in detail. For instance, Figure 4 reveals a pronounced seasonal
45 pattern, with INP concentrations peaking during the fall/winter months (October–January), particularly at warmer freezing
46 temperatures (e.g., $> -10^{\circ}\text{C}$). At colder temperatures (e.g., $\leq -15^{\circ}\text{C}$), the seasonal cycle is less distinct. Although INPs active
47 at the warmest temperatures ($\geq -6^{\circ}\text{C}$) were relatively rare, the few observed events tended to coincide with the fall/winter
48 peak. This site is influenced by surrounding agricultural activities, which may contribute to the observed seasonal variability
49 in INPs; however, a comprehensive source attribution is beyond the scope of this manuscript. Our intent here is to highlight
50 the completeness and continuity of the SGP dataset and its utility. These measurements support both observational studies of
51 INP variability and source characterization, and model evaluation efforts such as Knopf et al. (2021).

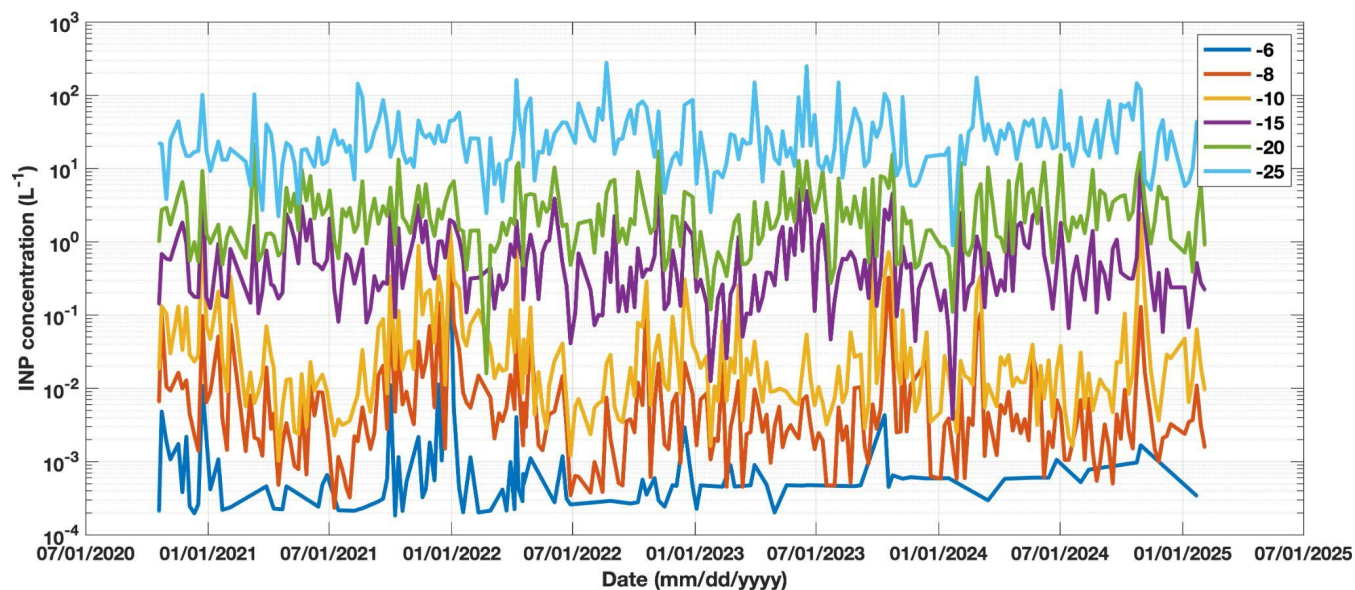


Figure 4: Complete time series of INP concentrations at select temperatures from the SGP C1 site that are currently publicly available on DOE ARM Data Discovery. Each line shows cumulative INP concentrations per liter of air (L^{-1}) at freezing temperatures designated in the legend (in $^{\circ}C$). Data are from 247 total processed filter samples.

4.2 Characterizing INP types through heat and peroxide treatments

In addition to the time series of total INP concentrations, approximately one-third of the samples undergo specific heat and peroxide treatments to help identify broad classes of INP types. These treatments target: (1) heat-labile INPs, such as proteins commonly associated with biological particles; (2) heat-stable organics, isolated via hydrogen peroxide treatment; and (3) the remaining, largely inorganic fraction, which is often attributed to mineral dust (Barry et al., 2023a, 2025; Creamean et al., 2020; DeMott et al., 2025a; Hill et al., 2016; McCluskey et al., 2018c; Schiebel et al., 2016; Suski et al., 2018; Testa et al., 2021; Tobo et al., 2019). Figure 5 provides an example of the relative contributions of these INP types over time at SGP C1, shown as a percentage of total INPs at two temperatures. The fraction of “biological” INPs is derived by subtracting the heat-treated INP spectrum from the untreated spectrum. The “organic” component is isolated by subtracting the peroxide-treated spectrum from the heat-treated spectrum. The residual “inorganic” fraction is estimated by subtracting the peroxide-treated spectrum from the untreated spectrum.

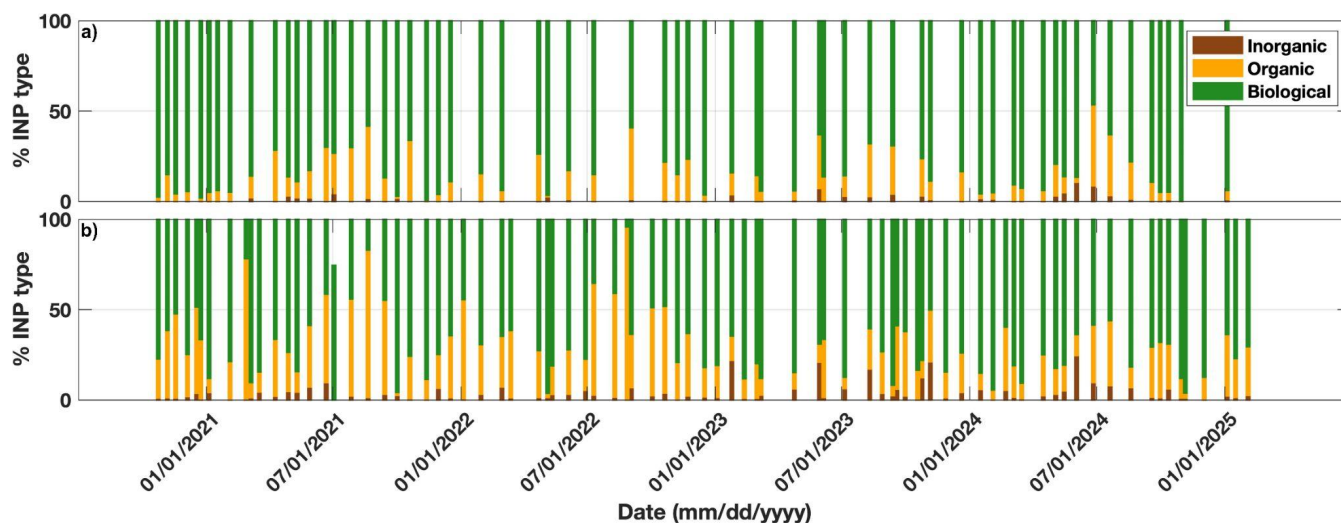


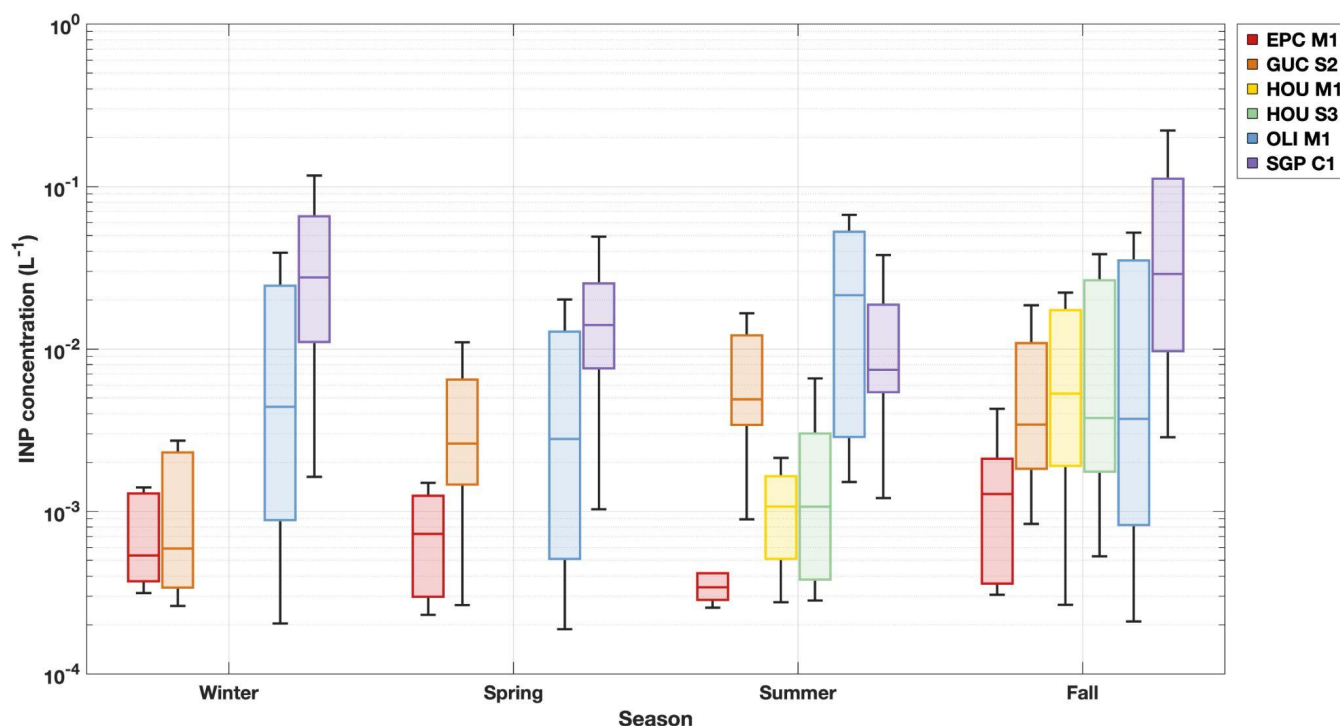
Figure 5: Relative abundance of INP type at the SGP C1 site at a) -15°C and b) -25°C that are currently available on DOE ARM Data Discovery. INP types are determined through heat and peroxide treatments. We assume that the reduction of INPs from heat are biological in nature (e.g., heat labile proteins) while the reduction of INPs from peroxide, UV, and heat are organic (e.g., heat labile organics). INPs remaining (unaffected) by both treatments are inorganic (e.g., mineral dust). Data are from 84 samples that have been heat- and peroxide-treated (34% of the processed SGP samples in Figure 4).

These unique long-term data offer insights into the seasonal variability and relative importance of different INP sources. For instance, at -15°C , biological INPs dominate at SGP, with smaller contributions from organics and inorganics. The inorganic component becomes more apparent during the summer months, likely associated with dry, dusty conditions on agricultural lands (Evans, 2025; Ginoux et al., 2012). At -25°C , the relative contributions of organic and inorganic INPs increase, yet biological INPs still remain the dominant type overall. Although the Great Plains region is periodically influenced by dust events, its agricultural soils are rich in biological material (Delgado-Baquerizo et al., 2018; Garcia et al., 2012; Hill et al., 2016; Kanji et al., 2017; O’Sullivan et al., 2014; Pereira et al., 2022; Steinke et al., 2016; Suski et al., 2018; Tobo et al., 2014), which distinguishes it from more arid, desert regions where mineral dust may dominate. These compositional insights are particularly valuable for users interested not only in INP abundance but also in potential sources. The treatment data can be used in combination with aerosol composition and meteorological observations at SGP C1 (and other ARM sites), and air mass trajectory analysis to further constrain the origins of INPs.

4.3 Seasonal INP variability across sites

INP data can be meaningfully compared across a diverse range of sites throughout the year, as illustrated in Figures 6 and 7 for -10°C and -20°C , respectively. The purpose of these figures is to highlight the diversity of INP concentrations across a range of environments and to demonstrate the value of consistent INP measurements at multiple sites. Each site shown represents a distinct setting: EPC M1 is a coastal marine site in California; GUC S2 is located at high elevation in the Colorado Rocky Mountains; the HOU sites include both urban and rural environments in Texas; OLI S3 is situated in a coastal oilfield region of northern Alaska within the Arctic; and SGP represents a high plains agricultural site in the central U.S. These are the

91 sites for which data are currently available through ARM Data Discovery, with additional datasets forthcoming for sites in
 92 Tasmania, northern Alaska, and the northeastern and southeastern United States.



93
 94 **Figure 6: Seasonal INP concentrations at -10°C at all fixed and mobile facility sites currently available from the DOE ARM Data**
 95 **Discovery.** Data are presented in box-and-whisker format, with the middle line being the median (50^{th} percentile), box edges representing
 96 the 25^{th} and 75^{th} percentiles, and the whiskers representing data within $1.5\times$ the interquartile range. The numbers above each median line
 97 indicate the number of data points that went into each bar.

98 Several noteworthy patterns emerge from these intercomparisons. At -10°C , where INPs are likely dominated by biological
 99 materials (Huang et al., 2021; Kanji et al., 2017), many sites exhibit clear seasonal cycles, though the timing and magnitude
 00 of these cycles differ. For instance, SGP shows elevated INP concentrations in the winter and fall, consistent with agricultural
 01 activity and associated emissions during that time. In contrast, GUC exhibits higher concentrations in summer, which aligns
 02 with the seasonal exposure of vegetation and the wintertime snow cover typical of the Colorado Rocky Mountains. Similarly,
 03 the Arctic coastal site OLI displays peak concentrations in summer, even exceeding those at the midlatitude SGP site. This is
 04 consistent with findings highlighting the biological productivity of Alaskan Arctic waters and tundra in May through
 05 September leading to increased airborne INPs (Barry et al., 2025; Creamean et al., 2018a, 2019; Eufemio et al., 2023; Fountain
 06 and Ohtake, 1985; Nieto-Caballero et al., 2025; Perring et al., 2023; Rogers et al., 2001; Wex et al., 2019), despite the presence
 07 of extensive oil and gas infrastructure near OLI that impacts the aerosol composition (Creamean et al., 2018b; Gunsch et al.,
 08 2017). However, a few important considerations should be noted. Field blanks were not collected at OLI; instead, a laboratory
 09 blank was used to subtract background INPs. This approach may lead to artificially elevated concentrations, as lab blanks

typically have lower background levels than field blanks due to reduced handling and exposure. Additionally, the OLI data represent a single summer season, whereas the SGP data span four summers. If the OLI summer was anomalous, this could skew comparisons. These factors should be carefully considered when interpreting or using the OLI dataset.

Conversely, EPC recorded the lowest INP concentrations among the sites, likely due to its exposure to clean marine air masses, which are generally associated with INP levels lower than terrestrial environments (e.g., DeMott et al., 2016; McCluskey et al., 2018b; Welti et al., 2020). Interestingly, both the urban and rural sites in HOU exhibited similar INP concentrations during the summer and fall, despite the common assumption that urban emissions are generally poor sources of INPs (Bi et al., 2019; Cabrera-Segoviano et al., 2022; Chen et al., 2018; Hasenkopf et al., 2016; Ren et al., 2023; Schrod et al., 2020; Tobo et al., 2020; Wagh et al., 2021; Yadav et al., 2019; Zhang et al., 2022; Zhao et al., 2019). The results from OLI and HOU collectively suggest that nearby regional marine sources can substantially influence INP concentrations, even in regions characterized by high levels of industrialization or urbanization.

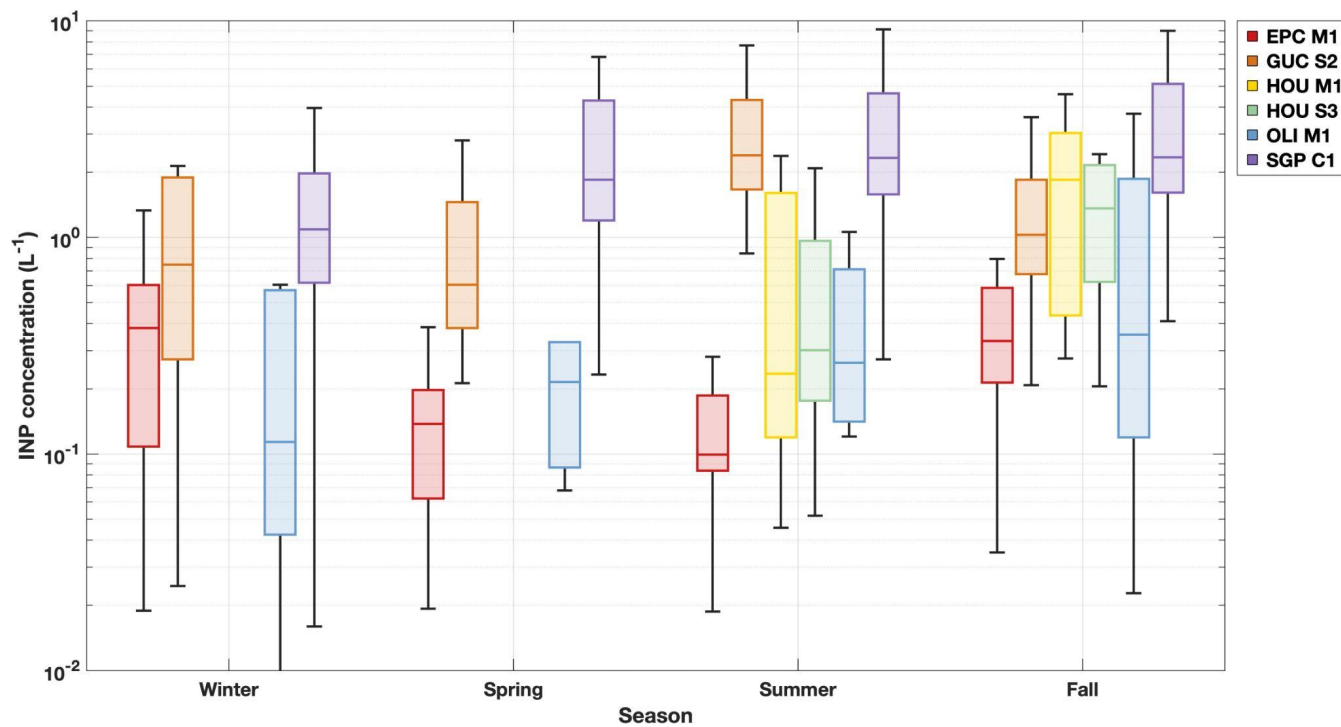


Figure 7: Same as Figure 6, but for seasonal INP concentrations at -20°C at all fixed and mobile facility sites currently available from the DOE ARM Data Discovery. Note the scale of the INP concentration axis is higher than Figure 6.

At -20°C , seasonal patterns in INP concentrations remain evident across most sites, but notable differences emerge compared to the -10°C data. INP concentrations at the two HOU sites remain comparable, consistent with the pattern observed at warmer temperatures. However, one of the most striking differences is that OLI, which had among the highest concentrations at $-$

27 10 °C, no longer stands out; instead, it shows significantly lower INP levels than SGP. This shift suggests that SGP may have
28 a more prominent source of mineral dust or cold-temperature-active organic INPs than the Arctic coastal OLI site. This
29 interpretation is consistent with known regional differences, as the U.S. midlatitudes, including the central plains where SGP
30 is located, coexist with more prominent dust emissions compared to the North American Arctic (e.g., Ginoux et al., 2012;
31 Rodriguez-Caballero et al., 2022; Song et al., 2021). Interestingly, INP concentrations at OLI are now more comparable to
32 those at EPC, likely reflecting the marine influence at both locations, which generally has lower INP concentrations relative
33 to continental sources.

34 These INP measurements are consistent with many principal investigator-led datasets collected at other ARM-supported
35 locations, such as those that employ the Colorado State University Ice Spectrometer (see Table 3). The INS that is used to
36 produce the ARM INP data is almost identical to the Ice Spectrometer. This opens opportunities for broader comparisons to
37 campaigns such as the 2017–2018 MARCUS (Measurements of Aerosols, Radiation, and Clouds over the Southern Ocean;
38 DeMott et al., 2018b; McCluskey et al., 2018c; McFarquhar et al., 2019, 2021; Niu et al., 2024; Raman et al., 2023) and 2016–
39 2018 MICRE (Macquarie Island Cloud and Radiation Experiment; DeMott et al., 2018a; Marchand, 2020; McCluskey et al.,
40 2023; Niu et al., 2024; Raman et al., 2023) campaigns in the Southern Ocean, 2019–2020 MOSAiC (Multidisciplinary drifting
41 Observatory for the Study of Arctic Climate; Barry et al., 2025; Creamean et al., 2022; Shupe et al., 2021, 2022) campaign in
42 the Arctic Ocean, 2019–2020 COMBLE (Cold-Air Outbreaks in the Marine Boundary Layer Experiment; DeMott and Hill,
43 2021; DeMott et al., 2025b; Geerts et al., 2021, 2022) campaign along the Norwegian Arctic coast, 2018–2019 CACTI (Cloud,
44 Aerosol, and Complex Terrain Interactions; DeMott and Hill, 2020; Testa et al., 2021; Varble et al., 2019) campaign in
45 agricultural regions of South America, the 2019 AEROICESTUDY (Aerosol-Ice Formation Closure Pilot Study; Knopf et al.,
46 2020, 2021) and 2014 INCE (Ice Nuclei Characterization Experiment; DeMott et al., 2015) at SGP, and the 2015 ACAPEX
47 (ARM Cloud Aerosol Precipitation Experiment; DeMott and Hill, 2016; Fan et al., 2014; Leung, 2016; Levin et al., 2019; Lin
48 et al., 2022) study off the coast of California. These complementary datasets are also publicly available through ARM Data
49 Discovery, but labeled as “icespec” (or “icespec-air” for aircraft measurements).

50 **Table 3. List of previous PI-led DOE ARM field campaigns with comparable INP data to the INS.** Includes measurement location,
51 start and end dates, filter collection details, and DOI for the INP measurements. Data from earlier studies do not have available DOIs. Note
52 all of these campaigns are AMF deployments. RV is abbreviated for Research Vessel.

Field campaign name	Location	INP filter start	INP filter end	Filter collection details	DOI (https://doi.org/)
Measurements of Aerosols, Radiation, and Clouds over the Southern Ocean (MARCUS)	Southern Ocean on the <i>Aurora Australis</i>	Oct 2017	Apr 2018	continuous; 24- to 48-h samples	10.5439/1638968
Macquarie Island Cloud and	Macquarie Island,	Mar	Mar 2018	continuous; 48- to	10.5439/1638330

Radiation Experiment (MICRE)	Australia	2016		72-h samples	
Multidisciplinary Drifting Observatory for the Study of Arctic Climate (MOSAIC)	Arctic Ocean on the <i>RV Polarstern</i>	Oct 2019	Oct 2020	continuous; 72-h samples	10.5439/1804484
Cold-Air Outbreaks in the Marine Boundary Layer Experiment (COMBLE)	Andenes, Norway	Dec 2019	Mar 2020	during CAOs; 6- to 74-h samples	10.5439/1755091
Cloud, Aerosol, and Complex Terrain Interactions (CACTI)	Villa Yacanto, Argentina	Oct 2018	Apr 2019	quasi-continuous; 8-h samples	10.5439/1607786
Cloud, Aerosol, and Complex Terrain Interactions (CACTI)	Sierras de Córdoba, Argentina	Nov 2018	Dec 2018	flight duration; various sample durations	10.5439/1607793
Aerosol-Ice Formation Closure Pilot Study (AEROICESTUDY)	SGP	Oct 2019	Oct 2019	continuous; 12- to 24-h samples	10.5439/1637710
Ice Nuclei Characterization Experiment (INCE)	SGP	Apr 2014	Jun 2014	continuous; 24-h samples	none
ARM Cloud Aerosol Precipitation Experiment (ACAPEX)	Pacific Ocean on the ARM G-1 aircraft	Jan 2015	Mar 2015	flight duration; 10-min to 3-h samples	none

5 Community use and limitations of ARM INP data

We present a comprehensive dataset of immersion mode INP concentrations from multiple sites across the United States and beyond. Most of these data are publicly available through the DOE ARM Data Discovery portal (<https://adc.arm.gov/discovery/>). On the portal, data from fixed sites and AMF deployments can be found by searching for “INP,” while data collected via ARM tethered balloon systems can be found by searching for “TBSINP.” DOIs for INP and TBSINP are <https://doi.org/10.5439/1770816> and <https://doi.org/10.5439/2001041>, respectively. For sites with ongoing measurements, data are routinely uploaded as batches of samples are processed using the INS. Upcoming INP datasets from the CAPE-k (KCG S3), CoURAGE (CRG M1 and S2), BNF (M1), and NSA (C1) sites will also be made available in the near future. These ARM-based INP measurements are directly comparable to other principal investigator-led datasets collected in previous studies at a wider range of locations, allowing for meaningful cross-site comparisons.

Importantly, duplicate filters are collected at most sites and preserved frozen for potential future analyses. Researchers interested in obtaining additional INP data on unprocessed samples or conducting their own supplementary aerosol physicochemical analyses can request these archived samples by submitting an ARM Small Campaign Request

68 (<https://www.arm.gov/guidance/campaign-guidelines/small-campaigns>) with the option to contact the ARM INP mentor team
69 (co-authors on this manuscript) with questions. At many of the sites listed in Table 1, only a subset of collected filters has been
70 processed to date. Therefore, users with specific dates or time periods of interest are encouraged to reach out to the mentor
71 team to request new analyses, including specialized treatments. A detailed filter collection log is available on the ARM INS
72 homepage (<https://www.arm.gov/capabilities/instruments/ins>) to help guide these inquiries. INP data from future campaigns
73 requested by researchers will also be made accessible to the broader research community.
74

75 The DOE ARM baseline INP measurements provide valuable long-term and IOP-based observations but have several
76 limitations that users should be aware of. First, these measurements do not account for time dependence in freezing behavior,
77 which is generally less significant than temperature dependence (Ervens and Feingold, 2013). Second, sampling assumes
78 collection of the total aerosol size distribution; however, this has not been explicitly tested, so the exact size range collected is
79 uncertain. The 0.2- μm filters we use have reduced transmission efficiency for particles around 150 nm (down to 65–78%), but
80 generally exhibit very high collection efficiency at most sizes (Spurny and Lodge, 1972). Third, because filters are collected
81 over 24 hours, typically every six days, short-term or episodic INP events may be missed, although higher-frequency sampling
82 can be requested. Fourth, these measurements are made at the surface and may not fully represent the INP population at cloud
83 level, though cloud-surface coupling analyses (e.g., Creamean et al., 2021; Griesche et al., 2021) and TBS INP data (Creamean
84 et al., 2025) can help bridge this gap. Lastly, not all samples are subjected to treatments unless requested, and, as noted by
85 Burrows et al. (2022), the absence of co-located baseline measurements of aerosol composition (particularly dust, sea spray,
86 and primary biological aerosol particles) limits the ability to fully constrain INP sources and improve parameterizations in
87 models.

88 **Data availability**

89 INP and TBSINP data are available from the DOE ARM Data Discovery portal (<https://adc.arm.gov/discovery/>) under DOIs
90 <https://doi.org/10.5439/1770816> (Creamean et al., 2024) and <https://doi.org/10.5439/2001041> (Creamean et al., 2025),
91 respectively.

92 **Author contributions**

93 JMC and AT conceptualised the INP mentor program. CCH and MV conducted the sample and data analysis for the INP data
94 that are publicly available for download from the DOE ARM Data Center. CCH and JMC were additionally responsible for
95 instrument installation and maintenance at the sites. All authors contributed to the writing of this manuscript.

96 **Competing interests**

97 None of the authors has any competing interests

98 **Disclaimer**

99 Publisher's note: Copernicus Publications remains neutral with regard to jurisdictional claims made in the text, published maps,
00 institutional affiliations, or any other geographical representation in this paper. While Copernicus Publications makes every
01 effort to include appropriate place names, the final responsibility lies with the authors.

02 **Acknowledgements**

03 This work was supported by the Office of Biological and Environmental Research within the U.S. Department of Energy
04 (DOE) through the Atmospheric Radiation Measurement (ARM) user facility. JMC, CCH, and MV received support under
05 DOE contract no. DE-0F-60173. We gratefully acknowledge James Mather for his invaluable support in the development and
06 implementation of the INP program. We also extend our sincere thanks to the ARM site staff for their significant assistance
07 with instrument installation, sample collection, and logistics. We gratefully acknowledge Thomas C. J. Hill for his foundational
08 role as co-mentor alongside JMC during the inception of this program, and for his enduring guidance and expertise. He is now
09 enjoying a well-earned retirement in Australia. ChatGPT was used to assist in editing and improving the wording of this
10 manuscript.

11 **Financial support**

12 This research has been supported by Argonne National Laboratory for the DOE under contract DE-0F-60173.

13 **References**

- 14 Agresti, A. and Coull, B. A.: Approximate Is Better than “Exact” for Interval Estimation of Binomial Proportions, *Am. Stat.*,
15 52, 119, <https://doi.org/10.2307/2685469>, 1998.
- 16 Barry, K. R., Hill, T. C. J., Jentsch, C., Moffett, B. F., Stratmann, F., and DeMott, P. J.: Pragmatic protocols for working
17 cleanly when measuring ice nucleating particles, *Atmospheric Res.*, 250, 105419,
18 <https://doi.org/10.1016/j.atmosres.2020.105419>, 2021.
- 19 Barry, K. R., Hill, T. C. J., Nieto-Caballero, M., Douglas, T. A., Kreidenweis, S. M., DeMott, P. J., and Creamean, J. M.:
20 Active thermokarst regions contain rich sources of ice-nucleating particles, *Atmospheric Chem. Phys.*, 23, 15783–15793,
21 <https://doi.org/10.5194/acp-23-15783-2023>, 2023a.
- 22 Barry, K. R., Hill, T. C. J., Moore, K. A., Douglas, T. A., Kreidenweis, S. M., DeMott, P. J., and Creamean, J. M.: Persistence

23 and Potential Atmospheric Ramifications of Ice-Nucleating Particles Released from Thawing Permafrost, *Environ. Sci.*
 24 *Technol.*, 57, 3505–3515, <https://doi.org/10.1021/acs.est.2c06530>, 2023b.

25 Barry, K. R., Hill, T. C. J., Kreidenweis, S., DeMott, P. J., Tobo, Y., and Creamean, J. M.: Bioaerosols as indicators of central
 26 Arctic ice nucleating particle sources, *Atmos Chem Phys Lett*, 2025.

27 Beall, C. M., Lucero, D., Hill, T. C., DeMott, P. J., Stokes, M. D., and Prather, K. A.: Best practices for precipitation sample
 28 storage for offline studies of ice nucleation in marine and coastal environments, *Atmospheric Meas. Tech.*, 13, 6473–6486,
 29 <https://doi.org/10.5194/amt-13-6473-2020>, 2020.

30 Beall, C. M., Hill, T. C. J., DeMott, P. J., Könemann, T., Pikridas, M., Drewnick, F., Harder, H., Pöhlker, C., Lelieveld, J.,
 31 Weber, B., Iakovides, M., Prokeš, R., Sciare, J., Andreae, M. O., Stokes, M. D., and Prather, K. A.: Ice-nucleating particles
 32 near two major dust source regions, *Atmospheric Chem. Phys.*, 22, 12607–12627, <https://doi.org/10.5194/acp-22-12607-2022>,
 33 2022.

34 Bi, K., McMeeking, G. R., Ding, D. P., Levin, E. J. T., DeMott, P. J., Zhao, D. L., Wang, F., Liu, Q., Tian, P., Ma, X. C.,
 35 Chen, Y. B., Huang, M. Y., Zhang, H. L., Gordon, T. D., and Chen, P.: Measurements of Ice Nucleating Particles in Beijing,
 36 China, *J. Geophys. Res. Atmospheres*, 124, 8065–8075, <https://doi.org/10.1029/2019JD030609>, 2019.

37 Burrows, S.: Agricultural Ice Nuclei at Southern Great Plains Supplemental Sampling (AGINSGP-SUPP) Field Campaign
 38 Report, 2023.

39 Burrows, S. M., McCluskey, C. S., Cornwell, G., Steinke, I., Zhang, K., Zhao, B., Zawadowicz, M., Raman, A., Kulkarni, G.,
 40 China, S., Zelenyuk, A., and DeMott, P. J.: Ice-Nucleating Particles That Impact Clouds and Climate: Observational and
 41 Modeling Research Needs, *Rev. Geophys.*, 60, e2021RG000745, <https://doi.org/10.1029/2021RG000745>, 2022.

42 Cabrera-Segoviano, D., Pereira, D. L., Rodriguez, C., Raga, G. B., Miranda, J., Alvarez-Ospina, H., and Ladino, L. A.: Inter-
 43 annual variability of ice nucleating particles in Mexico city, *Atmos. Environ.*, 273, 118964,
 44 <https://doi.org/10.1016/j.atmosenv.2022.118964>, 2022.

45 Chen, J., Wu, Z., Augustin-Bauditz, S., Grawe, S., Hartmann, M., Pei, X., Liu, Z., Ji, D., and Wex, H.: Ice-nucleating particle
 46 concentrations unaffected by urban air pollution in Beijing, China, *Atmospheric Chem. Phys.*, 18, 3523–3539,
 47 <https://doi.org/10.5194/acp-18-3523-2018>, 2018.

48 Conen, F., Morris, C. E., Leifeld, J., Yakutin, M. V., and Alewell, C.: Biological residues define the ice nucleation properties
 49 of soil dust, *Atmospheric Chem. Phys.*, 11, 9643–9648, <https://doi.org/10.5194/acp-11-9643-2011>, 2011.

50 Creamean, J., Hill, T., Hume, C., and Devadoss, T.: Ice Nucleation Spectrometer (INS) Instrument Handbook, U.S. Department
 51 of Energy, Atmospheric Radiation Measurement user facility, Richland, Washington, 2024.

52 Creamean, J. M., Suski, K. J., Rosenfeld, D., Cazorla, A., DeMott, P. J., Sullivan, R. C., White, A. B., Ralph, F. M., Minnis,
 53 P., Comstock, J. M., Tomlinson, J. M., and Prather, K. A.: Dust and Biological Aerosols from the Sahara and Asia Influence
 54 Precipitation in the Western U.S., *Science*, 339, 1572–1578, <https://doi.org/10.1126/science.1227279>, 2013.

55 Creamean, J. M., Kirpes, R. M., Pratt, K. A., Spada, N. J., Maahn, M., de Boer, G., Schnell, R. C., and China, S.: Marine and
 56 terrestrial influences on ice nucleating particles during continuous springtime measurements in an Arctic oilfield location,
 57 *Atmospheric Chem. Phys.*, 18, 18023–18042, <https://doi.org/10.5194/acp-18-18023-2018>, 2018a.

58 Creamean, J. M., Maahn, M., de Boer, G., McComiskey, A., Sedlacek, A. J., and Feng, Y.: The influence of local oil
 59 exploration and regional wildfires on summer 2015 aerosol over the North Slope of Alaska, *Atmospheric Chem. Phys.*, 18,

555–570, <https://doi.org/10.5194/acp-18-555-2018>, 2018b.

Creamean, J. M., Cross, J. N., Pickart, R., McRaven, L., Lin, P., Pacini, A., Hanlon, R., Schmale, D. G., Cenicerros, J., Aydele, T., Colombi, N., Bolger, E., and DeMott, P. J.: Ice nucleating particles carried from below a phytoplankton bloom to the Arctic atmosphere, *Geophys. Res. Lett.*, 46, 8572–8581, <https://doi.org/10.1029/2019GL083039>, 2019.

Creamean, J. M., Hill, T. C. J., DeMott, P. J., Uetake, J., Kreidenweis, S., and Douglas, T. A.: Thawing permafrost: an overlooked source of seeds for Arctic cloud formation, *Environ. Res. Lett.*, 15, 084022, <https://doi.org/10.1088/1748-9326/ab87d3>, 2020.

Creamean, J. M., de Boer, G., Telg, H., Mei, F., Dexheimer, D., Shupe, M. D., Solomon, A., and McComiskey, A.: Assessing the vertical structure of Arctic aerosols using balloon-borne measurements, *Atmospheric Chem. Phys.*, 21, 1737–1757, <https://doi.org/10.5194/acp-21-1737-2021>, 2021.

Creamean, J. M., Barry, K., Hill, T. C. J., Hume, C., DeMott, P. J., Shupe, M. D., Dahlke, S., Willmes, S., Schmale, J., Beck, I., Hoppe, C. J. M., Fong, A., Chamberlain, E., Bowman, J., Scharien, R., and Persson, O.: Annual cycle observations of aerosols capable of ice formation in central Arctic clouds, *Nat. Commun.*, 13, 3537, <https://doi.org/10.1038/s41467-022-31182-x>, 2022.

Creamean, J. M., Dexheimer, D., Hume, C. C., Vazquez, M., Hess, B. T. M., Longbottom, C. M., Ruiz, C. A., and Theisen, A. K.: Reaching new heights: A vertically-resolved ice nucleating particle sampler operating on Atmospheric Radiation Measurement (ARM) tethered balloon systems, *Atmos Meas Tech Discuss*, submitted, 2025.

Cziczo, D. J., Ladino, L., Boose, Y., Kanji, Z. A., Kupiszewski, P., Lance, S., Mertes, S., and Wex, H.: Measurements of Ice Nucleating Particles and Ice Residuals, <https://doi.org/10.1175/AMSMONOGRAPHS-D-16-0008.1>, 2017.

Daily, M. I., Tarn, M. D., Whale, T. F., and Murray, B. J.: An evaluation of the heat test for the ice-nucleating ability of minerals and biological material, *Atmospheric Meas. Tech.*, 15, 2635–2665, <https://doi.org/10.5194/amt-15-2635-2022>, 2022.

Delgado-Baquerizo, M., Oliverio, A. M., Brewer, T. E., Benavent-González, A., Eldridge, D. J., Bardgett, R. D., Maestre, F. T., Singh, B. K., and Fierer, N.: A global atlas of the dominant bacteria found in soil, *Science*, 359, 320–325, <https://doi.org/10.1126/science.aap9516>, 2018.

DeMott, P. and Hill, T.: COMBLE ARM Mobile Facility (AMF) Measurements of Ice Nucleating Particles Field Campaign Report, <https://doi.org/10.2172/1767118>, 2021.

DeMott, P., Hill, T., Suski, K., and Levin, E.: Southern Great Plains Ice Nuclei Characterization Experiment Final Campaign Summary, 2015.

DeMott, P., Hill, T. C., Marchand, R., and Alexander, S.: Macquarie Island Cloud and Radiation Experiment (MICRE) Ice Nucleating Particle Measurements Field Campaign Report, 2018a.

DeMott, P., Hill, T., and McFarquhar, G.: Measurements of Aerosols, Radiation, and Clouds over the Southern Ocean (MARCUS) Ice Nucleating Particle Measurements Field Campaign Report, 2018b.

DeMott, P. J.: An Exploratory Study of Ice Nucleation by Soot Aerosols, *J. Appl. Meteorol. Climatol.*, 29, 1072–1079, [https://doi.org/10.1175/1520-0450\(1990\)029%253C1072:AESOIN%253E2.0.CO;2](https://doi.org/10.1175/1520-0450(1990)029%253C1072:AESOIN%253E2.0.CO;2), 1990.

DeMott, P. J. and Hill, T. C.: ACAPEX – Ship-Based Ice Nuclei Collections Field Campaign Report, <https://doi.org/10.2172/1253893>, 2016.

96 DeMott, P. J. and Hill, T. C. J.: Cloud, Aerosol, and Complex Terrain Interactions (CACTI) ARM Aerial Facility (AAF)
97 Measurements of Ice Nucleating Particles Field Campaign Report, 2020.

98 DeMott, P. J., Hill, T. C. J., McCluskey, C. S., Prather, K. A., Collins, D. B., Sullivan, R. C., Ruppel, M. J., Mason, R. H.,
99 Irish, V. E., Lee, T., Hwang, C. Y., Rhee, T. S., Snider, J. R., McMeeking, G. R., Dhaniyala, S., Lewis, E. R., Wentzell, J. J.
00 B., Abbatt, J., Lee, C., Sultana, C. M., Ault, A. P., Axson, J. L., Diaz Martinez, M., Venero, I., Santos-Figueroa, G., Stokes,
01 M. D., Deane, G. B., Mayol-Bracero, O. L., Grassian, V. H., Bertram, T. H., Bertram, A. K., Moffett, B. F., and Franc, G. D.:
02 Sea spray aerosol as a unique source of ice nucleating particles, *Proc. Natl. Acad. Sci.*, 113, 5797–5803,
03 <https://doi.org/10.1073/pnas.1514034112>, 2016.

04 DeMott, P. J., Hill, T. C. J., Petters, M. D., Bertram, A. K., Tobo, Y., Mason, R. H., Suski, K. J., McCluskey, C. S., Levin, E.
05 J. T., Schill, G. P., Boose, Y., Rauker, A. M., Miller, A. J., Zaragoza, J., Rocci, K., Rothfuss, N. E., Taylor, H. P., Hader, J.
06 D., Chou, C., Huffman, J. A., Pöschl, U., Prenni, A. J., and Kreidenweis, S. M.: Comparative measurements of ambient
07 atmospheric concentrations of ice nucleating particles using multiple immersion freezing methods and a continuous flow
08 diffusion chamber, *Atmospheric Chem. Phys.*, 17, 11227–11245, <https://doi.org/10.5194/acp-17-11227-2017>, 2017.

09 DeMott, P. J., Mason, R. H., McCluskey, C. S., Hill, T. C. J., Perkins, R. J., Desyaterik, Y., Bertram, A. K., Trueblood, J. V.,
10 Grassian, V. H., Qiu, Y., Molinero, V., Tobo, Y., Sultana, C. M., Lee, C., and Prather, K. A.: Ice nucleation by particles
11 containing long-chain fatty acids of relevance to freezing by sea spray aerosols, *Environ. Sci. Process. Impacts*, 20, 1559–
12 1569, <https://doi.org/10.1039/C8EM00386F>, 2018c.

13 DeMott, P. J., Möhler, O., Cziczo, D. J., Hiranuma, N., Petters, M. D., Petters, S. S., Belosi, F., Bingemer, H. G., Brooks, S.
14 D., Budke, C., Burkert-Kohn, M., Collier, K. N., Danielczok, A., Eppers, O., Felgitsch, L., Garimella, S., Grothe, H., Herenz,
15 P., Hill, T. C. J., Höhler, K., Kanji, Z. A., Kiselev, A., Koop, T., Kristensen, T. B., Krüger, K., Kulkarni, G., Levin, E. J. T.,
16 Murray, B. J., Nicosia, A., O’Sullivan, D., Peckhaus, A., Polen, M. J., Price, H. C., Reicher, N., Rothenberg, D. A., Rudich,
17 Y., Santachiara, G., Schiebel, T., Schrod, J., Seifried, T. M., Stratmann, F., Sullivan, R. C., Suski, K. J., Szakáll, M., Taylor,
18 H. P., Ullrich, R., Vergara-Temprado, J., Wagner, R., Whale, T. F., Weber, D., Welti, A., Wilson, T. W., Wolf, M. J., and
19 Zenker, J.: The Fifth International Workshop on Ice Nucleation phase 2 (FIN-02): laboratory intercomparison of ice nucleation
20 measurements, *Atmospheric Meas. Tech.*, 11, 6231–6257, <https://doi.org/10.5194/amt-11-6231-2018>, 2018d.

21 DeMott, P. J., Hill, T. C. J., Moore, K. A., Perkins, R. J., Mael, L. E., Busse, H. L., Lee, H., Kaluarachchi, C. P., Mayer, K. J.,
22 Sauer, J. S., Mitts, B. A., Tivanski, A. V., Grassian, V. H., Cappa, C. D., Bertram, T. H., and Prather, K. A.: Atmospheric
23 oxidation impact on sea spray produced ice nucleating particles, *Environ. Sci. Atmospheres*, 3, 1513–1532,
24 <https://doi.org/10.1039/D3EA00060E>, 2023.

25 DeMott, P. J., Mirrieles, J. A., Petters, S. S., Cziczo, D. J., Petters, M. D., Bingemer, H. G., Hill, T. C. J., Froyd, K., Garimella,
26 S., Hallar, A. G., Levin, E. J. T., McCubbin, I. B., Perring, A. E., Rapp, C. N., Schiebel, T., Schrod, J., Suski, K. J., Weber,
27 D., Wolf, M. J., Zawadowicz, M., Zenker, J., Möhler, O., and Brooks, S. D.: Field intercomparison of ice nucleation
28 measurements: the Fifth International Workshop on Ice Nucleation Phase 3 (FIN-03), *Atmospheric Meas. Tech.*, 18, 639–672,
29 <https://doi.org/10.5194/amt-18-639-2025>, 2025a.

30 DeMott, P. J., Swanson, B. E., Creamean, J. M., Tobo, Y., Hill, T. C. J., Barry, K. R., Beck, I. F., Frietas, G. P., Heslin-Rees,
31 D., Lackner, C. P., Schmale, J., Krejci, R., Zieger, P., Geerts, B., and Kreidenweis, S. M.: Ice nucleating particle sources and
32 transports between the Central and Southern Arctic regions during winter cold air outbreaks, *Elem. Sci. Anthr.*, 13, 00063,
33 <https://doi.org/10.1525/elementa.2024.00063>, 2025b.

34 Després, Viviane R., Huffman, J. A., Burrows, S. M., Hoose, C., Safatov, Aleksandr S., Buryak, G., Fröhlich-Nowoisky, J.,
35 Elbert, W., Andreae, Meinrat O., Pöschl, U., and Jaenicke, R.: Primary biological aerosol particles in the atmosphere: a review,
36 *Tellus B Chem. Phys. Meteorol.*, 64, 15598, <https://doi.org/10.3402/tellusb.v64i0.15598>, 2012.

37 Dexheimer, D., Whitson, G., Cheng, Z., Sammon, J., Gaustad, K., Mei, F., and Longbottom, C.: Tethered Balloon System
38 (TBS) Instrument Handbook, <https://doi.org/10.2172/1415858>, 2024.

39 Ervens, B. and Feingold, G.: Sensitivities of immersion freezing: Reconciling classical nucleation theory and deterministic
40 expressions, *Geophys. Res. Lett.*, 40, 3320–3324, <https://doi.org/10.1002/grl.50580>, 2013.

41 Eufemio, R. J., de Almeida Ribeiro, I., Sformo, T. L., Laursen, G. A., Molinero, V., Fröhlich-Nowoisky, J., Bonn, M., and
42 Meister, K.: Lichen species across Alaska produce highly active and stable ice nucleators, *Biogeosciences*, 20, 2805–2812,
43 <https://doi.org/10.5194/bg-20-2805-2023>, 2023.

44 Evans, S.: Dust-producing weather patterns of the North American Great Plains, *Atmospheric Chem. Phys.*, 25, 4833–4845,
45 <https://doi.org/10.5194/acp-25-4833-2025>, 2025.

46 Fan, J., Leung, L. R., DeMott, P. J., Comstock, J. M., Singh, B., Rosenfeld, D., Tomlinson, J. M., White, A., Prather, K. A.,
47 Minnis, P., Ayers, J. K., and Min, Q.: Aerosol impacts on California winter clouds and precipitation during CalWater 2011:
48 local pollution versus long-range transported dust, *Atmospheric Chem. Phys.*, 14, 81–101, [https://doi.org/10.5194/acp-14-81-](https://doi.org/10.5194/acp-14-81-2014)
49 2014, 2014.

50 Feldman, D. R., Aiken, A. C., Boos, W. R., Carroll, R. W. H., Chandrasekar, V., Collis, S., Creamean, J. M., Boer, G. de,
51 Deems, J., DeMott, P. J., Fan, J., Flores, A. N., Gochis, D., Grover, M., Hill, T. C. J., Hodshire, A., Hulm, E., Hume, C. C.,
52 Jackson, R., Junyent, F., Kennedy, A., Kumjian, M., Levin, E. J. T., Lundquist, J. D., O'Brien, J., Raleigh, M. S., Reithel, J.,
53 Rhoades, A., Rittger, K., Rudisill, W., Sherman, Z., Siirila-Woodburn, E., Skiles, S. M., Smith, J. N., Sullivan, R. C., Theisen,
54 A., Tuftedal, M., Varble, A. C., Wiedlea, A., Wielandt, S., Williams, K., and Xu, Z.: The Surface Atmosphere Integrated Field
55 Laboratory (SAIL) Campaign, <https://doi.org/10.1175/BAMS-D-22-0049.1>, 2023.

56 Fountain, A. G. and Ohtake, T.: Concentrations and Source Areas of Ice Nuclei in the Alaskan Atmosphere, *J. Clim. Appl.*
57 *Meteorol.*, 24, 377–382, [https://doi.org/10.1175/1520-0450\(1985\)024%253C0377:CASAOI%253E2.0.CO;2](https://doi.org/10.1175/1520-0450(1985)024%253C0377:CASAOI%253E2.0.CO;2), 1985.

58 Garcia, E., Hill, T. C. J., Prenni, A. J., DeMott, P. J., Franc, G. D., and Kreidenweis, S. M.: Biogenic ice nuclei in boundary
59 layer air over two U.S. High Plains agricultural regions, *J. Geophys. Res. Atmospheres*, 117,
60 <https://doi.org/10.1029/2012JD018343>, 2012.

61 Geerts, B., McFarquhar, G., Xue, L., Jensen, M., Kollias, P., Ovchinnikov, M., Shupe, M., DeMott, P., Wang, Y., Tjernstrom,
62 M., Field, P., Abel, S., Spengler, T., Neggers, R., Crewell, S., Wendisch, M., and Lupkes, C.: Cold-Air Outbreaks in the Marine
63 Boundary Layer Experiment (COMBLE) Field Campaign Report, <https://doi.org/10.2172/1763013>, 2021.

64 Geerts, B., Giangrande, S. E., McFarquhar, G. M., Xue, L., Abel, S. J., Comstock, J. M., Crewell, S., DeMott, P. J., Ebell, K.,
65 Field, P., Hill, T. C. J., Hunzinger, A., Jensen, M. P., Johnson, K. L., Juliano, T. W., Kollias, P., Kosovic, B., Lackner, C.,
66 Luke, E., Lüpkes, C., Matthews, A. A., Neggers, R., Ovchinnikov, M., Powers, H., Shupe, M. D., Spengler, T., Swanson, B.
67 E., Tjernström, M., Theisen, A. K., Wales, N. A., Wang, Y., Wendisch, M., and Wu, P.: The COMBLE Campaign: A Study
68 of Marine Boundary Layer Clouds in Arctic Cold-Air Outbreaks, *Bull. Am. Meteorol. Soc.*, 103, E1371–E1389,
69 <https://doi.org/10.1175/BAMS-D-21-0044.1>, 2022.

70 Ginoux, P., Prospero, J. M., Gill, T. E., Hsu, N. C., and Zhao, M.: Global-scale attribution of anthropogenic and natural dust
71 sources and their emission rates based on MODIS Deep Blue aerosol products, *Rev. Geophys.*, 50,
72 <https://doi.org/10.1029/2012RG000388>, 2012.

73 Gratzl, J., Böhmländer, A., Pätsi, S., Pogner, C.-E., Gorfer, M., Brus, D., Doulgeris, K. M., Wieland, F., Asmi, E., Saarto, A.,
74 Möhler, O., Stolzenburg, D., and Grothe, H.: Locally emitted fungal spores serve as high temperature ice nucleating particles
75 in the European sub-Arctic, *EGUsphere*, 1–38, <https://doi.org/10.5194/egusphere-2025-1599>, 2025.

76 Griesche, H. J., Ohneiser, K., Seifert, P., Radenz, M., Engelmann, R., and Ansmann, A.: Contrasting ice formation in Arctic
77 clouds: surface-coupled vs. surface-decoupled clouds, *Atmospheric Chem. Phys.*, 21, 10357–10374,
78 <https://doi.org/10.5194/acp-21-10357-2021>, 2021.

79 Gunsch, M. J., Kirpes, R. M., Kolesar, K. R., Barrett, T. E., China, S., Sheesley, R. J., Laskin, A., Wiedensohler, A., Tuch, T.,
80 and Pratt, K. A.: Contributions of transported Prudhoe Bay oil field emissions to the aerosol population in Utqiagvik, Alaska,
81 *Atmospheric Chem. Phys.*, 17, 10879–10892, <https://doi.org/10.5194/acp-17-10879-2017>, 2017.

82 Gute, E. and Abbatt, J. P. D.: Ice nucleating behavior of different tree pollen in the immersion mode, *Atmos. Environ.*, 231,
83 117488, <https://doi.org/10.1016/j.atmosenv.2020.117488>, 2020.

84 Hasenkopf, C. A., Veghte, D. P., Schill, G. P., Lodoysamba, S., Freedman, M. A., and Tolbert, M. A.: Ice nucleation, shape,
85 and composition of aerosol particles in one of the most polluted cities in the world: Ulaanbaatar, Mongolia, *Atmos. Environ.*,
86 139, 222–229, <https://doi.org/10.1016/j.atmosenv.2016.05.037>, 2016.

87 Hill, T. C. J., DeMott, P. J., Tobo, Y., Fröhlich-Nowoisky, J., Moffett, B. F., Franc, G. D., and Kreidenweis, S. M.: Sources
88 of organic ice nucleating particles in soils, *Atmospheric Chem. Phys.*, 16, 7195–7211, [https://doi.org/10.5194/acp-16-7195-](https://doi.org/10.5194/acp-16-7195-2016)
89 2016, 2016.

90 Hill, T. C. J., Malfatti, F., McCluskey, C. S., Schill, G. P., Santander, M. V., Moore, K. A., Rauker, A. M., Perkins, R. J.,
91 Celussi, M., Levin, E. J. T., Suski, K. J., Cornwell, G. C., Lee, C., Negro, P. D., Kreidenweis, S. M., Prather, K. A., and
92 DeMott, P. J.: Resolving the controls over the production and emission of ice-nucleating particles in sea spray, *Environ. Sci.*
93 *Atmospheres*, 3, 970–990, <https://doi.org/10.1039/D2EA00154C>, 2023.

94 Hoose, C. and Möhler, O.: Heterogeneous ice nucleation on atmospheric aerosols: a review of results from laboratory
95 experiments, *Atmospheric Chem. Phys.*, 12, 9817–9854, <https://doi.org/10.5194/acp-12-9817-2012>, 2012.

96 Huang, S., Hu, W., Chen, J., Wu, Z., Zhang, D., and Fu, P.: Overview of biological ice nucleating particles in the atmosphere,
97 *Environ. Int.*, 146, 106197, <https://doi.org/10.1016/j.envint.2020.106197>, 2021.

98 Janine Fröhlich-Nowoisky, Kampf, C. J., Weber, B., Huffman, J. A., Pöhlker, C., Andreae, M. O., Lang-Yona, N., Burrows,
99 S. M., Gunthe, S. S., Elbert, W., Su, H., Hoor, P., Thines, E., Hoffmann, T., Després, V. R., and Pöschl, U.: Bioaerosols in the
00 Earth system: Climate, health, and ecosystem interactions, *Atmospheric Res.*, 182, 346–376,
01 <https://doi.org/10.1016/j.atmosres.2016.07.018>, 2016.

02 Jensen, M., Flynn, J., Kollias, P., Kuang, C., McFarquhar, G., Powers, H., Brooks, S., Bruning, E., Collins, D., Collis, S., Fan,
03 J., Fridlind, A., Giangrande, S., Griffin, R., Hu, J., Jackson, R., Kumjian, M., Logan, T., Matsui, T., Nowotarski, C., Oue, M.,
04 Rapp, A., Rosenfeld, D., Ryzhkov, A., Sheesley, R., Snyder, J., Stier, P., Usenko, S., Van Den Heever, S., Van Lier-Walqui,
05 M., Varble, A., Wang, Y., Aiken, A., Deng, M., Dexheimer, D., Dubey, M., Feng, Y., Ghate, V., Johnson, K., Lamer, K.,
06 Saleeby, S., Wang, D., Zawadowicz, M., and Zhou, A.: Tracking Aerosol Convection Interactions Experiment (TRACER)
07 Field Campaign Report, <https://doi.org/10.2172/2202672>, 2023.

08 Kanji, Z. A., Ladino, L. A., Wex, H., Boose, Y., Burkert-Kohn, M., Cziczo, D. J., and Krämer, M.: Overview of ice nucleating
09 particles, *Meteor Monogr*, 58, 1.1-1.33, <https://doi.org/10.1175/AMSMONOGRAPHS-D-16-0006.1>, 2017.

10 Kaufmann, L., Marcolli, C., Hofer, J., Pinti, V., Hoyle, C. R., and Peter, T.: Ice nucleation efficiency of natural dust samples
11 in the immersion mode, *Atmospheric Chem. Phys.*, 16, 11177–11206, <https://doi.org/10.5194/acp-16-11177-2016>, 2016.

12 Knopf, D. A. and Alpert, P. A.: Atmospheric ice nucleation, *Nat. Rev. Phys.*, 5, 203–217, [https://doi.org/10.1038/s42254-023-](https://doi.org/10.1038/s42254-023-00570-7)
13 00570-7, 2023.

Knopf, D. A., DeMott, P., Creamean, J., Riemer, N., Hiranuma, N., Laskin, A., Sullivan, R., Fridlind, A., Liu, X., West, M., and Hill, T.: Aerosol-Ice Formation Closure Pilot Study (AEROICESTUDY) Field Campaign Report, 2020.

Knopf, D. A., Barry, K. R., Brubaker, T. A., Jahl, L. G., Jankowski, K. A., Li, J., Lu, Y., Monroe, L. W., Moore, K. A., Rivera-Adorno, F. A., Saucedo, K. A., Shi, Y., Tomlin, J. M., Vepuri, H. S. K., Wang, P., Lata, N. N., Levin, E. J. T., Creamean, J. M., Hill, T. C. J., China, S., Alpert, P. A., Moffet, R. C., Hiranuma, N., Sullivan, R. C., Fridlind, A. M., West, M., Riemer, N., Laskin, A., DeMott, P. J., and Liu, X.: Aerosol–Ice Formation Closure: A Southern Great Plains Field Campaign, *Bull. Am. Meteorol. Soc.*, 102, E1952–E1971, <https://doi.org/10.1175/BAMS-D-20-0151.1>, 2021.

Lacher, L., Adams, M. P., Barry, K., Bertozzi, B., Bingemer, H., Boffo, C., Bras, Y., Büttner, N., Castarede, D., Cziczo, D. J., DeMott, P. J., Fösig, R., Goodell, M., Höhler, K., Hill, T. C. J., Jentsch, C., Ladino, L. A., Levin, E. J. T., Mertes, S., Möhler, O., Moore, K. A., Murray, B. J., Nadolny, J., Pfeuffer, T., Picard, D., Ramírez-Romero, C., Ribeiro, M., Richter, S., Schrod, J., Sellegri, K., Stratmann, F., Swanson, B. E., Thomson, E. S., Wex, H., Wolf, M. J., and Freney, E.: The Puy de Dôme Ice Nucleation Intercomparison Campaign (PICNIC): comparison between online and offline methods in ambient air, *Atmospheric Chem. Phys.*, 24, 2651–2678, <https://doi.org/10.5194/acp-24-2651-2024>, 2024.

Leung, L. R.: ARM Cloud-Aerosol-Precipitation Experiment (ACAPEX) Field Campaign Report, U.S. Department of Energy, Office of Science, Office of Biological and Environmental Research, 2016.

Levin, E. J. T., McMeeking, G. R., Carrico, C. M., Mack, L. E., Kreidenweis, S. M., Wold, C. E., Moosmüller, H., Arnott, W. P., Hao, W. M., Collett Jr., J. L., and Malm, W. C.: Biomass burning smoke aerosol properties measured during Fire Laboratory at Missoula Experiments (FLAME), *J. Geophys. Res. Atmospheres*, 115, <https://doi.org/10.1029/2009JD013601>, 2010.

Levin, E. J. T., DeMott, P. J., Suski, K. J., Boose, Y., Hill, T. C. J., McCluskey, C. S., Schill, G. P., Rocci, K., Al-Mashat, H., Kristensen, L. J., Cornwell, G., Prather, K., Tomlinson, J., Mei, F., Hubbe, J., Pekour, M., Sullivan, R., Leung, L. R., and Kreidenweis, S. M.: Characteristics of Ice Nucleating Particles in and Around California Winter Storms, *J. Geophys. Res. Atmospheres*, 124, 11530–11551, <https://doi.org/10.1029/2019JD030831>, 2019.

Lin, Y., Fan, J., Li, P., Leung, L. R., DeMott, P. J., Goldberger, L., Comstock, J., Liu, Y., Jeong, J.-H., and Tomlinson, J.: Modeling impacts of ice-nucleating particles from marine aerosols on mixed-phase orographic clouds during 2015 ACAPEX field campaign, *Atmospheric Chem. Phys.*, 22, 6749–6771, <https://doi.org/10.5194/acp-22-6749-2022>, 2022.

Maki, L. R., Galyan, E. L., Chang-Chien, M.-M., and Caldwell, D. R.: Ice Nucleation Induced by *Pseudomonas syringae*1, *Appl. Microbiol.*, 28, 456–459, 1974.

Marchand, R.: Macquarie Island Cloud and Radiation Experiment (MICRE) Field Campaign Report, <https://doi.org/10.2172/1602536>, 2020.

McCluskey, C. S., Hill, T. C. J., Malfatti, F., Sultana, C. M., Lee, C., Santander, M. V., Beall, C. M., Moore, K. A., Cornwell, G. C., Collins, D. B., Prather, K. A., Jayarathne, T., Stone, E. A., Azam, F., Kreidenweis, S. M., and DeMott, P. J.: A Dynamic Link between Ice Nucleating Particles Released in Nascent Sea Spray Aerosol and Oceanic Biological Activity during Two Mesocosm Experiments, *J. Atmospheric Sci.*, 74, 151–166, <https://doi.org/10.1175/JAS-D-16-0087.1>, 2017.

McCluskey, C. S., Hill, T. C. J., Sultana, C. M., Laskina, O., Trueblood, J., Santander, M. V., Beall, C. M., Michaud, J. M., Kreidenweis, S. M., Prather, K. A., Grassian, V., and DeMott, P. J.: A mesocosm double feature: Insights into the chemical makeup of marine ice nucleating particles, *J. Atmospheric Sci.*, 75, 2405–2423, <https://doi.org/10.1175/JAS-D-17-0155.1>, 2018a.

McCluskey, C. S., Ovadnevaite, J., Rinaldi, M., Atkinson, J., Belosi, F., Ceburnis, D., Marullo, S., Hill, T. C. J., Lohmann, U., Kanji, Z. A., O’Dowd, C., Kreidenweis, S. M., and DeMott, P. J.: Marine and terrestrial organic ice-nucleating particles in

53 pristine marine to continentally influenced Northeast Atlantic air masses, *J. Geophys. Res. Atmospheres*, 123, 6196–6212,
54 <https://doi.org/10.1029/2017JD028033>, 2018b.

55 McCluskey, C. S., Hill, T. C. J., Humphries, R. S., Rauker, A. M., Moreau, S., Stratton, P. G., Chambers, S. D., Williams, A.
56 G., McRobert, I., Ward, J., Keywood, M. D., Harnwell, J., Ponsonby, W., Loh, Z. M., Krummel, P. B., Protat, A., Kreidenweis,
57 S. M., and DeMott, P. J.: Observations of ice nucleating particles over Southern Ocean waters, *Geophys. Res. Lett.*, 45, 11,989–
58 11,997, <https://doi.org/10.1029/2018GL079981>, 2018c.

59 McCluskey, C. S., Gettelman, A., Bardeen, C. G., DeMott, P. J., Moore, K. A., Kreidenweis, S. M., Hill, T. C. J., Barry, K.
60 R., Twohy, C. H., Toohey, D. W., Rainwater, B., Jensen, J. B., Reeves, J. M., Alexander, S. P., and McFarquhar, G. M.:
61 Simulating Southern Ocean aerosol and ice nucleating particles in the Community Earth System Model version 2, *J. Geophys.*
62 *Res. Atmospheres*, 128, e2022JD036955, <https://doi.org/10.1029/2022JD036955>, 2023.

63 McFarquhar, G., Marchand, R., Bretherton, C., Alexander, S., Protat, A., Siems, S., Wood, R., and DeMott, P.: Measurements
64 of Aerosols, Radiation, and Clouds Over the Southern Ocean (MARCUS) Field Campaign Report, 2019.

65 McFarquhar, G. M., Bretherton, C. S., Marchand, R., Protat, A., DeMott, P. J., Alexander, S. P., Roberts, G. C., Twohy, C.
66 H., Toohey, D., Siems, S., Huang, Y., Wood, R., Rauber, R. M., Lasher-Trapp, S., Jensen, J., Stith, J. L., Mace, J., Um, J.,
67 Järvinen, E., Schnaiter, M., Gettelman, A., Sanchez, K. J., McCluskey, C. S., Russell, L. M., McCoy, I. L., Atlas, R. L.,
68 Bardeen, C. G., Moore, K. A., Hill, T. C. J., Humphries, R. S., Keywood, M. D., Ristovski, Z., Cravigan, L., Schofield, R.,
69 Fairall, C., Mallet, M. D., Kreidenweis, S. M., Rainwater, B., D'Alessandro, J., Wang, Y., Wu, W., Saliba, G., Levin, E. J. T.,
70 Ding, S., Lang, F., Truong, S. C. H., Wolff, C., Haggerty, J., Harvey, M. J., Klekociuk, A. R., and McDonald, A.: Observations
71 of clouds, aerosols, precipitation, and surface radiation over the Southern Ocean: An overview of CAPRICORN, MARCUS,
72 MICRE, and SOCRATES, *Bull. Am. Meteorol. Soc.*, 102, E894–E928, <https://doi.org/10.1175/BAMS-D-20-0132.1>, 2021.

73 McLean, W.: The Nature of Soil Organic Matter as Shown by the attack of Hydrogen Peroxide, *J. Agric. Sci.*, 21, 595–611,
74 <https://doi.org/10.1017/S0021859600009813>, 1931.

75 Mikutta, R., Kleber, M., Kaiser, K., and Jahn, R.: Review: Organic Matter Removal from Soils using Hydrogen Peroxide,
76 Sodium Hypochlorite, and Disodium Peroxodisulfate, *Soil Sci. Soc. Am. J.*, 69, 120–135,
77 <https://doi.org/10.2136/sssaj2005.0120>, 2005.

78 Moore, K. A., Hill, T. C. J., Madawala, C. K., Leibensperger III, R. J., Greeney, S., Cappa, C. D., Stokes, M. D., Deane, G.
79 B., Lee, C., Tivanski, A. V., Prather, K. A., and DeMott, P. J.: Wind-driven emission of marine ice-nucleating particles in the
80 Scripps Ocean-Atmosphere Research Simulator (SOARS), *Atmospheric Chem. Phys.*, 25, 3131–3159,
81 <https://doi.org/10.5194/acp-25-3131-2025>, 2025.

82 Nieto-Caballero, M., Barry, K. R., Hill, T. C. J., Douglas, T. A., DeMott, P. J., Kreidenweis, S. M., and Creamean, J. M.:
83 Airborne bacteria over thawing permafrost landscapes in the Arctic, *Environ. Sci. Technol.*, 59, 9027–9036,
84 <https://doi.org/10.1021/acs.est.4c11774>, 2025.

85 Niu, Q., McFarquhar, G. M., Marchand, R., Theisen, A., Cavallo, S. M., Flynn, C., DeMott, P. J., McCluskey, C. S.,
86 Humphries, R. S., and Hill, T. C. J.: 62°S Witnesses the Transition of Boundary Layer Marine Aerosol Pattern Over the
87 Southern Ocean (50°S–68°S, 63°E–150°E) During the Spring and Summer: Results From MARCUS (I), *J. Geophys. Res.*
88 *Atmospheres*, 129, e2023JD040396, <https://doi.org/10.1029/2023JD040396>, 2024.

89 O’Sullivan, D., Murray, B. J., Malkin, T. L., Whale, T. F., Umo, N. S., Atkinson, J. D., Price, H. C., Baustian, K. J., Browse,
90 J., and Webb, M. E.: Ice nucleation by fertile soil dusts: relative importance of mineral and biogenic components, *Atmospheric*
91 *Chem. Phys.*, 14, 1853–1867, <https://doi.org/10.5194/acp-14-1853-2014>, 2014.

92 O’Sullivan, D., Murray, B. J., Ross, J. F., and Webb, M. E.: The adsorption of fungal ice-nucleating proteins on mineral dusts:
93 a terrestrial reservoir of atmospheric ice-nucleating particles, *Atmospheric Chem. Phys.*, 16, 7879–7887,
94 <https://doi.org/10.5194/acp-16-7879-2016>, 2016.

95 Pereira, D. L., Gavilán, I., Letechipía, C., Raga, G. B., Puig, T. P., Mugica-Álvarez, V., Alvarez-Ospina, H., Rosas, I.,
96 Martinez, L., Salinas, E., Quintana, E. T., Rosas, D., and Ladino, L. A.: Mexican agricultural soil dust as a source of ice
97 nucleating particles, *Atmospheric Chem. Phys.*, 22, 6435–6447, <https://doi.org/10.5194/acp-22-6435-2022>, 2022.

98 Pereira Freitas, G., Adachi, K., Conen, F., Heslin-Rees, D., Krejci, R., Tobo, Y., Yttri, K. E., and Zieger, P.: Regionally sourced
99 bioaerosols drive high-temperature ice nucleating particles in the Arctic, *Nat. Commun.*, 14, 5997,
00 <https://doi.org/10.1038/s41467-023-41696-7>, 2023.

01 Perkins, R. J., Gillette, S. M., Hill, T. C. J., and DeMott, P. J.: The Labile Nature of Ice Nucleation by Arizona Test Dust, *ACS*
02 *Earth Space Chem.*, 4, 133–141, <https://doi.org/10.1021/acsearthspacechem.9b00304>, 2020.

03 Perring, A. E., Mediavilla, B., Wilbanks, G. D., Churnside, J. H., Marchbanks, R., Lamb, K. D., and Gao, R.-S.: Airborne
04 bioaerosol observations imply a strong terrestrial source in the summertime Arctic, *J. Geophys. Res. Atmospheres*, 128,
05 e2023JD039165, <https://doi.org/10.1029/2023JD039165>, 2023.

06 Raman, A., Hill, T., DeMott, P. J., Singh, B., Zhang, K., Ma, P.-L., Wu, M., Wang, H., Alexander, S. P., and Burrows, S. M.:
07 Long-term variability in immersion-mode marine ice-nucleating particles from climate model simulations and observations,
08 *Atmospheric Chem. Phys.*, 23, 5735–5762, <https://doi.org/10.5194/acp-23-5735-2023>, 2023.

09 Ren, Y. Z., Bi, K., Fu, S. Z., Tian, P., Huang, M. Y., Zhu, R. H., and Xue, H. W.: The Relationship of Aerosol Properties and
10 Ice-Nucleating Particle Concentrations in Beijing, *J. Geophys. Res. Atmospheres*, 128, e2022JD037383,
11 <https://doi.org/10.1029/2022JD037383>, 2023.

12 Robinson, G. W.: Note on the mechanical analysis of humus soils, *J. Agric. Sci.*, 12, 287–291,
13 <https://doi.org/10.1017/S0021859600005347>, 1922.

14 Rodriguez-Caballero, E., Stanelle, T., Egerer, S., Cheng, Y., Su, H., Canton, Y., Belnap, J., Andreae, M. O., Tegen, I., Reick,
15 C. H., Pöschl, U., and Weber, B.: Global cycling and climate effects of aeolian dust controlled by biological soil crusts, *Nat.*
16 *Geosci.*, 15, 458–463, <https://doi.org/10.1038/s41561-022-00942-1>, 2022.

17 Rogers, D. C., DeMott, P. J., and Kreidenweis, S. M.: Airborne measurements of tropospheric ice-nucleating aerosol particles
18 in the Arctic spring, *J. Geophys. Res. Atmospheres*, 106, 15053–15063, <https://doi.org/10.1029/2000JD900790>, 2001.

19 Roy, P., Mael, L. E., Hill, T. C. J., Mehndiratta, L., Peiker, G., House, M. L., DeMott, P. J., Grassian, V. H., and Dutcher, C.
20 S.: Ice Nucleating Activity and Residual Particle Morphology of Bulk Seawater and Sea Surface Microlayer, *ACS Earth Space*
21 *Chem.*, 5, 1916–1928, <https://doi.org/10.1021/acsearthspacechem.1c00175>, 2021.

22 Russell, L. M., Lubin, D., Silber, I., Eloranta, E., Muelmenstaedt, J., Burrows, S., Aiken, A., Wang, D., Petters, M., Miller,
23 M., Ackerman, A., Fridlind, A., Witte, M., Lebsock, M., Painemal, D., Chang, R., Liggio, J., and Wheeler, M.: EPCAPE Field
24 Campaign Final Campaign Report April, 2024.

25 Schiebel, T., Höhler, K., Funk, R., Hill, T. C. J., Levin, E. J. T., Nadolny, J., Steinke, I., Suski, K. J., Ullrich, R., Wagner, R.,
26 Weber, I., DeMott, P. J., and Möhler, O.: Ice nucleation activity of various agricultural soil dust aerosol particles, *European*
27 *Geosciences Union General Assembly*, Wien, A, April 17-22, 2016. *Geophysical Research Abstracts*, 18(2016) EGU2016-
28 13422, 2016.

- 29 Schneider, J., Höhler, K., Heikkilä, P., Keskinen, J., Bertozzi, B., Bogert, P., Schorr, T., Umo, N. S., Vogel, F., Brasseur, Z.,
30 Wu, Y., Hakala, S., Duplissy, J., Moiseev, D., Kulmala, M., Adams, M. P., Murray, B. J., Korhonen, K., Hao, L., Thomson,
31 E. S., Castarède, D., Leisner, T., Petäjä, T., and Möhler, O.: The seasonal cycle of ice-nucleating particles linked to the
32 abundance of biogenic aerosol in boreal forests, *Atmospheric Chem. Phys.*, 21, 3899–3918, [https://doi.org/10.5194/acp-21-](https://doi.org/10.5194/acp-21-3899-2021)
33 3899-2021, 2021.
- 34 Schnell, R. C. and Vali, G.: Biogenic Ice Nuclei: Part I. Terrestrial and Marine Sources, *J. Atmospheric Sci.*, 33, 1554–1564,
35 [https://doi.org/10.1175/1520-0469\(1976\)033%253C1554:BINPIT%253E2.0.CO;2](https://doi.org/10.1175/1520-0469(1976)033%253C1554:BINPIT%253E2.0.CO;2), 1976.
- 36 Schrod, J., Thomson, E. S., Weber, D., Kossmann, J., Pöhlker, C., Saturno, J., Ditas, F., Artaxo, P., Clouard, V., Saurel, J.-M.,
37 Ebert, M., Curtius, J., and Bingemer, H. G.: Long-term deposition and condensation ice-nucleating particle measurements
38 from four stations across the globe, *Atmospheric Chem. Phys.*, 20, 15983–16006, <https://doi.org/10.5194/acp-20-15983-2020>,
39 2020.
- 40 Schultz, M. K., Biegalski, S. R., Inn, K. G. W., Yu, L., Burnett, W. C., Thomas, J. L. W., and Smith, G. E.: Optimizing the
41 removal of carbon phases in soils and sediments for sequential chemical extractions by coulometry, *J. Environ. Monit.*, 1, 183–
42 190, <https://doi.org/10.1039/A900534J>, 1999.
- 43 Sequi, P. and Aringhieri, R.: Destruction of Organic Matter by Hydrogen Peroxide in the Presence of Pyrophosphate and Its
44 Effect on Soil Specific Surface Area, *Soil Sci. Soc. Am. J.*, 41, 340–342,
45 <https://doi.org/10.2136/sssaj1977.03615995004100020033x>, 1977.
- 46 Shupe, M., Chu, D., Costa, D., Cox, C., Creamean, J., De Boer, G., Dethloff, K., Engelmann, R., Gallagher, M., Hunke, E.,
47 Maslowski, W., McComiskey, A., Osborn, J., Persson, O., Powers, H., Pratt, K., Randall, D., Solomon, A., Tjernstrom, M.,
48 Turner, D., Uin, J., Uttal, T., Verlinde, J., and Wagner, D.: Multidisciplinary drifting Observatory for the Study of Arctic
49 Climate (MOSAiC) (Field Campaign Report), <https://doi.org/10.2172/1787856>, 2021.
- 50 Shupe, M. D., Rex, M., Blomquist, B., Persson, P. O. G., Schmale, J., Uttal, T., Althausen, D., Angot, H., Archer, S., Bariteau,
51 L., Beck, I., Bilberry, J., Bucci, S., Buck, C., Boyer, M., Brasseur, Z., Brooks, I. M., Calmer, R., Cassano, J., Castro, V., Chu,
52 D., Costa, D., Cox, C. J., Creamean, J., Crewell, S., Dahlke, S., Damm, E., de Boer, G., Deckelmann, H., Dethloff, K., Dütsch,
53 M., Ebell, K., Ehrlich, A., Ellis, J., Engelmann, R., Fong, A. A., Frey, M. M., Gallagher, M. R., Ganzeveld, L., Gradinger, R.,
54 Graeser, J., Greenamyer, V., Griesche, H., Griffiths, S., Hamilton, J., Heinemann, G., Helmig, D., Herber, A., Heuzé, C.,
55 Hofer, J., Houchens, T., Howard, D., Inoue, J., Jacobi, H.-W., Jaiser, R., Jokinen, T., Jourdan, O., Jozef, G., King, W.,
56 Kirchgassner, A., Klingebiel, M., Krassovski, M., Krumpen, T., Lampert, A., Landing, W., Laurila, T., Lawrence, D.,
57 Lonardi, M., Loose, B., Lüpkes, C., Maahn, M., Macke, A., Maslowski, W., Marsay, C., Maturilli, M., Mech, M., Morris, S.,
58 Moser, M., Nicolaus, M., Ortega, P., Osborn, J., Pätzold, F., Perovich, D. K., Petäjä, T., Pilz, C., Pirazzini, R., Posman, K.,
59 Powers, H., Pratt, K. A., Preußner, A., Quéléver, L., Radenz, M., Rabe, B., Rinke, A., Sachs, T., Schulz, A., Siebert, H., Silva,
60 T., Solomon, A., et al.: Overview of the MOSAiC expedition: *Atmosphere, Elem. Sci. Anthr.*, 10, 00060,
61 <https://doi.org/10.1525/elementa.2021.00060>, 2022.
- 62 Song, Q., Zhang, Z., Yu, H., Ginoux, P., and Shen, J.: Global dust optical depth climatology derived from CALIOP and
63 MODIS aerosol retrievals on decadal timescales: regional and interannual variability, *Atmospheric Chem. Phys.*, 21, 13369–
64 13395, <https://doi.org/10.5194/acp-21-13369-2021>, 2021.
- 65 Spurny, K. R. and Lodge, J. P.: Collection Efficiency Tables for Membrane Filters Used in the Sampling and Analysis of
66 Aerosols and Hydrosols, Laboratory of Atmospheric Science, National Center for Atmospheric Research, 56 pp., 1972.
- 67 Steinke, I., Funk, R., Busse, J., Iturri, A., Kirchen, S., Leue, M., Möhler, O., Schwartz, T., Schnaiter, M., Sierau, B., Toprak,
68 E., Ullrich, R., Ulrich, A., Hoose, C., and Leisner, T.: Ice nucleation activity of agricultural soil dust aerosols from Mongolia,
69 Argentina, and Germany, *J. Geophys. Res. Atmospheres*, 121, 13,559–13,576, <https://doi.org/10.1002/2016JD025160>, 2016.

70 Suski, K. J., Hill, T. C. J., Levin, E. J. T., Miller, A., DeMott, P. J., and Kreidenweis, S. M.: Agricultural harvesting emissions
71 of ice-nucleating particles, *Atmospheric Chem. Phys.*, 18, 13755–13771, <https://doi.org/10.5194/acp-18-13755-2018>, 2018.

72 Teska, C. J., Dieser, M., and Foreman, C. M.: Clothing Textiles as Carriers of Biological Ice Nucleation Active Particles,
73 *Environ. Sci. Technol.*, 58, 6305–6312, <https://doi.org/10.1021/acs.est.3c09600>, 2024.

74 Testa, B., Hill, T. C. J., Marsden, N. A., Barry, K. R., Hume, C. C., Bian, Q., Uetake, J., Hare, H., Perkins, R. J., Möhler, O.,
75 Kreidenweis, S. M., and DeMott, P. J.: Ice Nucleating Particle Connections to Regional Argentinian Land Surface Emissions
76 and Weather During the Cloud, Aerosol, and Complex Terrain Interactions Experiment, *J. Geophys. Res. Atmospheres*, 126,
77 <https://doi.org/10.1029/2021JD035186>, 2021.

78 Tobo, Y., DeMott, P. J., Hill, T. C. J., Prenni, A. J., Swoboda-Colberg, N. G., Franc, G. D., and Kreidenweis, S. M.: Organic
79 matter matters for ice nuclei of agricultural soil origin, *Atmospheric Chem. Phys.*, 14, 8521–8531, [https://doi.org/10.5194/acp-](https://doi.org/10.5194/acp-14-8521-2014)
80 [14-8521-2014](https://doi.org/10.5194/acp-14-8521-2014), 2014.

81 Tobo, Y., Adachi, K., DeMott, P. J., Hill, T. C. J., Hamilton, D. S., Mahowald, N. M., Nagatsuka, N., Ohata, S., Uetake, J.,
82 Kondo, Y., and Koike, M.: Glacially sourced dust as a potentially significant source of ice nucleating particles, *Nat. Geosci.*,
83 12, 253–258, <https://doi.org/10.1038/s41561-019-0314-x>, 2019.

84 Tobo, Y., Uetake, J., Matsui, H., Moteki, N., Uji, Y., Iwamoto, Y., Miura, K., and Misumi, R.: Seasonal Trends of Atmospheric
85 Ice Nucleating Particles Over Tokyo, *J. Geophys. Res. Atmospheres*, 125, e2020JD033658,
86 <https://doi.org/10.1029/2020JD033658>, 2020.

87 Vali, G.: Quantitative Evaluation of Experimental Results an the Heterogeneous Freezing Nucleation of Supercooled Liquids,
88 *J. Atmospheric Sci.*, 28, 402–409, [https://doi.org/10.1175/1520-0469\(1971\)028%253C0402:QEOERA%253E2.0.CO;2](https://doi.org/10.1175/1520-0469(1971)028%253C0402:QEOERA%253E2.0.CO;2), 1971.

89 Vali, G., Christensen, M., Fresh, R. W., Galyan, E. L., Maki, L. R., and Schnell, R. C.: Biogenic Ice Nuclei. Part II: Bacterial
90 Sources, *J. Atmospheric Sci.*, 33, 1565–1570, [https://doi.org/10.1175/1520-](https://doi.org/10.1175/1520-0469(1976)033%253C1565:BINPIB%253E2.0.CO;2)
91 [0469\(1976\)033%253C1565:BINPIB%253E2.0.CO;2](https://doi.org/10.1175/1520-0469(1976)033%253C1565:BINPIB%253E2.0.CO;2), 1976.

92 Varble, A., Nesbitt, S., Salio, P., Avila, E., Borque, P., McFarquhar, G., Van Den Heever, S., Zipser, E., Gochis, D., Houze
93 Jr., R., Jensen, M., Kollias, P., Kreidenweis, S., Leung, R., Rasmussen, K., Romps, D., Williams, C., and DeMott, P.: Cloud,
94 Aerosol, and Complex Terrain Interactions (CACTI) Field Campaign Report, <https://doi.org/10.2172/1574024>, 2019.

95 Wagh, S., Singh, P., Ghude, S. D., Safai, P., Prabhakaran, T., and Kumar, P. P.: Study of ice nucleating particles in fog-haze
96 weather at New Delhi, India: A case of polluted environment, *Atmospheric Res.*, 259, 105693,
97 <https://doi.org/10.1016/j.atmosres.2021.105693>, 2021.

98 Welti, A., Bigg, E. K., DeMott, P. J., Gong, X., Hartmann, M., Harvey, M., Henning, S., Herenz, P., Hill, T. C. J., Hornblow,
99 B., Leck, C., Löffler, M., McCluskey, C. S., Rauker, A. M., Schmale, J., Tatzelt, C., Van Pinxteren, M., and Stratmann, F.:
00 Ship-based measurements of ice nuclei concentrations over the Arctic, Atlantic, Pacific and Southern oceans, *Atmospheric*
01 *Chem. Phys.*, 20, 15191–15206, <https://doi.org/10.5194/acp-20-15191-2020>, 2020.

02 Wex, H., Augustin-Bauditz, S., Boose, Y., Budke, C., Curtius, J., Diehl, K., Dreyer, A., Frank, F., Hartmann, S., Hiranuma,
03 N., Jantsch, E., Kanji, Z. A., Kiselev, A., Koop, T., Möhler, O., Niedermeier, D., Nillius, B., Rösch, M., Rose, D., Schmidt,
04 C., Steinke, I., and Stratmann, F.: Intercomparing different devices for the investigation of ice nucleating particles using
05 Snomax^{&sup>}®^{&sup>} as test substance, *Atmospheric Chem. Phys.*, 15, 1463–1485, [https://doi.org/10.5194/acp-](https://doi.org/10.5194/acp-15-1463-2015)
06 [15-1463-2015](https://doi.org/10.5194/acp-15-1463-2015), 2015.

07 Wex, H., Huang, L., Zhang, W., Hung, H., Traversi, R., Becagli, S., Sheesley, R. J., Moffett, C. E., Barrett, T. E., Bossi, R.,

- 08 Skov, H., Hünnerbein, A., Lubitz, J., Löffler, M., Linke, O., Hartmann, M., Herenz, P., and Stratmann, F.: Annual variability
09 of ice-nucleating particle concentrations at different Arctic locations, *Atmospheric Chem. Phys.*, 19, 5293–5311,
10 <https://doi.org/10.5194/acp-19-5293-2019>, 2019.
- 11 Yadav, S., Venezia, R. E., Paerl, R. W., and Petters, M. D.: Characterization of Ice-Nucleating Particles Over Northern India,
12 *J. Geophys. Res. Atmospheres*, 124, 10467–10482, <https://doi.org/10.1029/2019JD030702>, 2019.
- 13 Zhang, C., Wu, Z., Chen, J., Chen, J., Tang, L., Zhu, W., Pei, X., Chen, S., Tian, P., Guo, S., Zeng, L., Hu, M., and Kanji, Z.
14 A.: Ice-nucleating particles from multiple aerosol sources in the urban environment of Beijing under mixed-phase cloud
15 conditions, *Atmospheric Chem. Phys.*, 22, 7539–7556, <https://doi.org/10.5194/acp-22-7539-2022>, 2022.
- 16 Zhao, B., Wang, Y., Gu, Y., Liou, K.-N., Jiang, J. H., Fan, J., Liu, X., Huang, L., and Yung, Y. L.: Ice nucleation by aerosols
17 from anthropogenic pollution, *Nat. Geosci.*, 12, 602–607, <https://doi.org/10.1038/s41561-019-0389-4>, 2019.